CZECH TECHNICAL
UNIVERSITY
IN PRAGUE

F3

Faculty of Electrical Engineering
Department of Circuit Theory

Master's Thesis

Intelligent Cell Spray System

Jan Andrys
Medical electronics and bioinformatics

May 2023
Inteligentní rozprašovač kožních buněk
Supervisor: prof. Quan Zhou, Ing. Jan Havlík, Ph.D

MASTER'S THESIS ASSIGNMENT

I. Personal and study details

Student's name: **Andrys Jan** Personal ID number: **474437**

Faculty / Institute: **Faculty of Electrical Engineering**

Department / Institute: **Department of Circuit Theory**

Study program: **Medical Electronics and Bioinformatics**

Specialisation: **Medical Instrumentation**

II. Master's thesis details

Master's thesis title in English:

Intelligent Cell Spray System

Master's thesis title in Czech:

Inteligentní rozprašovač kožních buněk

Guidelines:

The project aims to design, build and test a hand-robotic device for burn surgery. The device is used for burned wound skin cell spray-painting therapy. It will help surgeons with the uniform distribution of cell medication by measuring the distance between the sprayer and the body wound, speed of movement, and angle between the sprayer and the body. All these parameters are important to present to the surgeon in real-time. Additionally, a dispensing system for cell medication will be developed.
Guidelines:
1. Design and test several measuring methods and choose the best one for the prototype.
2. Design the dispensing system which is compatible with the current air system.
3. Build and validate the prototype, which is possible to use during surgery.
4. Write proper software which ensures smooth and easy use.

Bibliography / sources:

[1] C. Albitar, P. Graebling, and C. Doignon, “Robust Structured Light Coding for 3D Reconstruction”, IEEE, 2007.
[2] S. Izadi, A. Davison, A. Fitzgibbon, D. Kim, O. Hilliges, D. Molyneaux, R. Newcombe, P. Kohli, J. Shotton, S. Hodges, and D. Freeman, “KinectFusion”, in Proceedings of the 24th annual ACM symposium on User interface software and technology - UIST '11, 2011, p. 559-.
[3] J. M. Pearce and B. Wijnen, “Open-source syringe pump”, Appropedia, 2016.
[4] I. Z. Ibragimov and I. M. Afanasyev, "Comparison of ROS-based visual SLAM methods in homogeneous indoor environment," 2017 14th Workshop on Positioning, Navigation and Communications (WPNC), 2017, pp. 1-6, doi: 10.1109/WPNC.2017.8250081.

Name and workplace of master's thesis supervisor:

prof. Quan Zhou Aalto University, Finland

Name and workplace of second master's thesis supervisor or consultant:

Ing. Jan Havlík, Ph.D. Department of Circuit Theory, FEE

Date of master's thesis assignment: **09.12.2022** Deadline for master's thesis submission: **26.05.2023**

Assignment valid until: **22.09.2024**

prof. Quan Zhou Supervisor's signature	doc. Ing. Radoslav Bortel, Ph.D. Head of department's signature	prof. Mgr. Petr Páta, Ph.D. Dean's signature

Acknowledgement / Declaration

I would like to thank my family for their intensive support during my studies. I appreciate my supervisors prof. Quan Zhou, Dr Esko Kankuri, Ph.D, and Ing. Jan Havlik, Ph.D for willingness, help, given consultations and opportunity to work on this project.

I declare that the presented work was developed independently and that I have listed all sources of information used within it in accordance with methodical instructions for observing the ethical principles in the preparation of university theses.

In Prague, 25.5.2023

....

Abstrakt / Abstract

Tato práce popisuje proces vývoje inteligentního rozprašovače kožních buněk používaného pro léčbu různých druhů popálenin. Hlavním úkolem zařízení je rovnoměrné rozdělení léčivé látky po popálenině. Práce diskutuje několik možností řešení takového problému, mezi které patří odhad rychlosti pohybu zařízení při nástřiku nebo určení absolutní polohy vůči tělu pacienta. Právě poslední možnost řešení se jeví jako nejlepší z ohledem na kvalitu postřiku, navíc nabízí další benefity které pomůžou vývoji léčivé látky. Je ovšem potřeba vyřešit i další problémy spojené s požadavky operace, například dodržení stejné vzdálenosti mezi tělem pacienta a aplikátorem, nebo možnost použít zařízení jednoduše bez předchozího školení. Během projektu byli postaveny dva prototypy, při jejich vývoji byli jednotlivé problémy diskutovány s chirurgy, kteří poskytli svůj pohled odborníka na danou problematiku, zároveň přesně definovali problémy, které by toto zařízení mělo vyřešit.

Klíčová slova: Popáleniny, Měření vzdálenosti, Měření rychlosti, Lineární motor, 3D skenování, OpenCV

Překlad titulu: Inteligentní rozprašovač kožních buněk

This thesis describes the process of developing an intelligent skin cell sprayer used to treat various types of burns. The main task of the device is to distribute the therapeutic substance over the burn evenly. Several possible solutions are described for such a problem which include estimating the speed of movement of the device during application and determining the absolute position relative to the patient's body. The second solution seems to be ideal in terms of spray quality and offers additional benefits that will help develop the therapeutic substance. However, other issues related to the operation requirements need to be addressed, such as maintaining a consistent distance between the patient's body and the applicator. Or perhaps the ability to use the device easily and effectively without prior training. During the project, two prototypes were built. Individual problems were discussed with surgeons, who provided expert perspectives on the issue and precisely defined the problems that this device should solve.

Keywords: Burns, Distance measuring, Speed measuring, Linear stage, 3D scanning, Spraying, OpenCV, Motion estimation, Cell therapies

Contents

Chapter 1
Introduction

All of us have suffered from a burn at some point, but in most cases, it was just a first-degree burn that is painful but can be healed in a few days. However, higher-degree burns require proper treatment, especially the third and fourth degrees. Patients with these burns often need a substitution of the skin affected by the burn. The most common treatment is skin grafting [1]. Skin is removed from a non-burnt part of the body and placed on the cleaned wound. The donor skin can mesh to cover larger wound areas. The second method is called skin substitutes or cell therapies. It is still a new and researched method with a big potential to change the way severe burns are healed. This method delivers proteins, skin-grown factors, and stem cells using a vehicle or matrix on the wound [2]. It is applied by spraying said parts with a vehicle on the wound in a controlled way.

One of the cell therapies in burn surgeries was developed at the University of Helsinki by a research group led by Dr Esko Kankuri. They faced problems with the repeatability of delivering the mentioned medication on the wound. The application has to meet several requirements to accomplish a high-quality treatment. Among these requirements is keeping the same distance between the nozzle of the sprayer and the body wound during the application process, and the main requirement is the uniform distribution of the medication around the wound area.

As of right now, the medication is used in experimental mode, and it is applied by surgeons without any specialized tools. It is simply pressing the medication liquid out of the syringes and trying to keep all requirements for applying. Although every surgeon has a different approach to achieving it.

The applying method has a strong potential to be automatized. The task is to standardize the applying method and make it more available even for surgeons without specialized training. Solving the problem and achieving the goal is a complex task with no straightforward solution. The goals of the thesis are a) to evaluate current measurement distance measurement methods, b) to design a proof-of-the-concept device for controlled application of medication to burn wounds

This thesis is focused only on the applying methods and the medication will not be covered in the thesis. The main question is ”How to reliably measure the distance and motion of the device during application using sensors and estimation algorithms?”. To answer this it is necessary to separate the tasks and compare individual solutions.

In the end, gathered information will be combined and used to develop a prototype that exhibits that such a device is beneficial and can help surgeons with the application.

During the work, contact with clinicians was maintained to create a prototype that is not just a testing device but has practical properties for use in real medical environments.

Chapter 2
Background

2.1 Skin burn therapy

Burns are common skin injuries with high variability levels of seriousness. Four types of burns are determined according to the depth of damaged skin. For understanding burns it is important to know some information about skin.

The skin is composed of three main layers. The upper layer is the epidermis, which provides waterproofing and a barrier to infection. The second layer is called dermis, it contains fibroblast, elastin, collagen, nerve fibers and more components which supports the skin and ensures the resistance against stress and strain. The last layer is sometimes called hypodermis or subcutis. Blood vessels which provides oxygen and nutriens are part of it. It also contains sweat gland, and fat. The lowest layer (hypodermis) is connected to the fibrous tissue of the bones and muscles [3].

The burn types are called degrees, the first-degree burn is not a severe injury, and just the epidermis is damaged. Second-degree burns often need proper treatment, and higher degrees require even special care in burn centers [4–5]. But it is also important to know size of the burn, it is common to use parameter TBSA (total body surface area) which says in percentage the burn parts of the body. According to the method, surface of palm and fingers is equal to 1% of TBSA.

Problems connected with burn can be reduced by suitable diagnostics. And correct depth of the burn have to be estimated for proper treatment. Following methods can be used:

- Digital Imaging
- Biopsy
- Laser Doppler techniques
- Photo-Optical Measurement
- Ultrasound

Severe burns often requires skin replacement. The list bellow shows the most common method:

- Skin Graft
- Keratinocyte Culture

The skin grafting method is still the most common. During the surgery, part of the healthy skin is taken and placed on the cleaned burn wound. The issue is that the method increases the TBSA affected.

The Keratinocyte culture is also called cell therapy and there are different types of such a treatment. One example, aims to replace tissues with cultured cells. This method does not require a large donor site. On the other hand, the time for regrowth is long and it can take several weeks [6].

2.2 Commercial medical spraying devices

There are several competitors on the market which are trying to solve a problem similar to this, spraying some type of medication on damaged wounds.

Competitors does not provide:

- feedback during application
- application speed control
- dose control
- on-wound visualization
- on-wound volumetric control

Here is list of the main competitors. Next subsections briefly describes the key technological differences in the spraying procedure and the applicator. The treatment parameters are not discussed.

- RECELL®
- SpinCare ™
- RenovaCare SkinGun ™
- Baxter EasySpray ™

2.2.1 ReCell

The ReCell® system was introduced into clinical practice in 2005 to replace the gold standard of skin graft replacements and it uses the cell based method for healing thermal burn wounds. During the procedure, just a small donor site is needed for covering large wounds (1:80 - 1 cm^2 of biopsy to cover up to 80 cm^2 of damaged area). It uses the enzyme Trypsin to produce cells such as keratinocytes, melanocytes, Langerhand cells, and fibroblasts. These cells are suspended in a lactate solution and by using a syringe with a special end sprayed on the damaged wound [7–8].

The spraying procedure is the main issue of this method, there is no control over the amount of the cells applied to the wound.

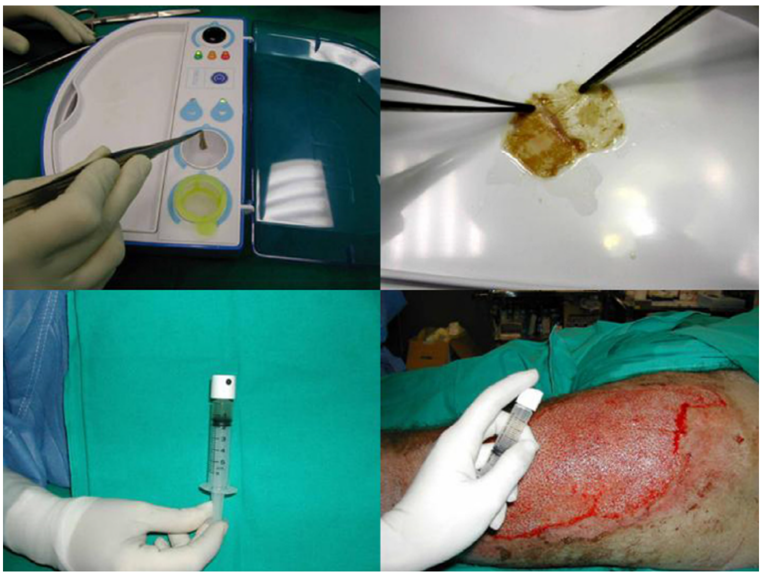

Figure 2.1. ReCell® procedure [8]

2.2.2 SpinCare

SpinCare ™ is an electrospinning wound treatment device. It is a hand-held, battery-operated, portable device. It prints the Spincare ™ matrix which behaves as a temporary skin substitute. Additionally, it is possible to add healing supplements into the nanofibres [9].

Figure 2.2. SpinCare ™ device [10]

This device is very similar to what this thesis is trying to study and produce. It contains a motorized stage that pushes the medication out of syringes and it also contains distance measurement. The overall design is clever, it is two-button controlled and battery-powered. This solution provides the right device which can be used as an inspiration for our new device.

But similar to the previous device, it does not provide dose control. From practice and recommendations, it is possible to know that for example, one full syringe will cover A4 damaged area. However, that is not enough for proper treatment. But SpinCare ™ produces nanofibres that are white right after application the surgeon can estimate the layer of applied medication easier than with colorless liquids.

In the image 2.3 bellow it is possible to see how the SpinCare ™ looks under the cover.

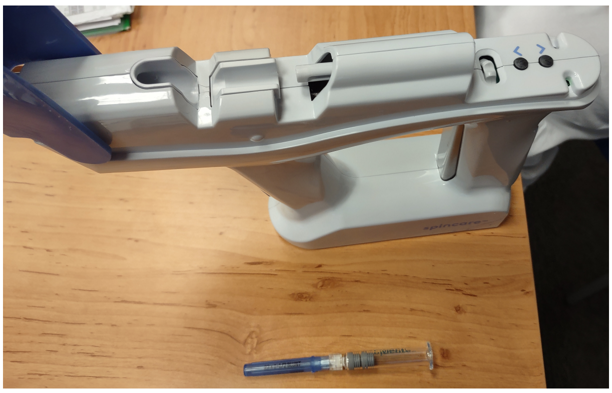

Figure 2.3. Inside of the SpinCare ™ device

2.2.3 RenovaCare SkinGun

The solution made by the company RenovaCare is similar to the ReCell® system. It also uses cell therapy to heal burns, chronics, and acute wounds. RenovaCare paid more attention to the application of the medication in comparison to ReCell® because they developed a specialized spraying device the SkinGun ™ which applies the medication CellMist ™ on the wound.

The SkinGun ™ is similar to the device which this thesis is trying to develop, it contains a linear stage that pushes the syringe with medication and also provides an air pressure regulator which is used for spraying cells without damaging them.

According to the RenovaCare web page, the SkinGun ™ achieves 97.3% cell viability and uniform coverage is 200 times greater than the conventional methods. But there is no dose control and the whole process is based on the experience of surgeons.

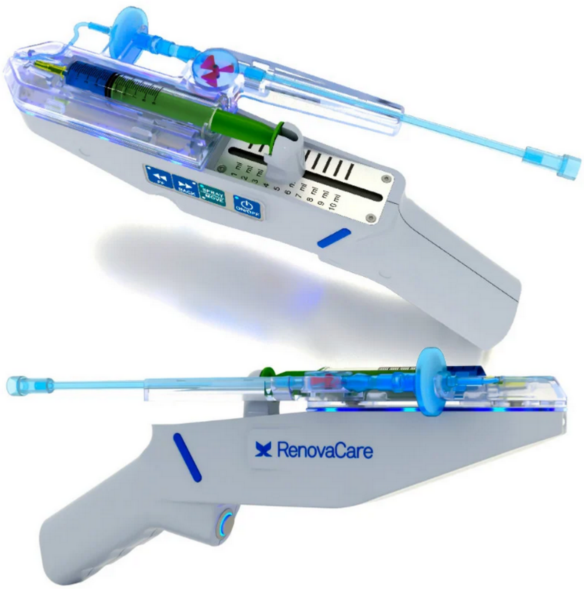

Figure 2.4. RenovaCare SkinGun ™ device [11]

2.2.4 Baxter EasySpray

Baxter EasySpray ™ is a pressure regulator which can be used with a specialized nozzle as a sprayer of cell based medication. This device is currently used at the University of Helsinki Hospital for testing cell based medication. The uncontrolled way of applying was the main trigger for designing a new specialized device and creating this project and thesis.

The device can change the pressure for therapy and uses on/off button for controlling the air flow. But as was explained in the current solution 5.1.1 subsection there is no feedback for the surgeons that they are following all requirements during the application process. The application procedure which uses Baxter EasySpray ™ is visible in image 5.1

Figure 2.5. Baxter Easy spray, original purpose [12]

2.3 Motion estimation

Most of the task of this thesis can be solved by motion estimation and motion tracking. When the position of the sprayer is known in real space or at least according to the body of the patient, it is not hard to estimate the distance between the sprayer and the body. The position estimation has to be calculated in real-time so it is also possible to calculate the speed of movement. But it is important to keep in mind the size of the device.

For a small handheld device, a combination of visual-based motion estimation and inertial measurement units (IMUs) would be a suitable choice. This combination can provide accurate and robust motion estimation while keeping the hardware requirements manageable.

2.3.1 Visual-based motion estimation

One of the options is visual-based motion estimation. It utilizes the camera or image sensor on the handheld device to estimate motion. Optical flow algorithms [13] can be employed to track the displacement of pixels between consecutive frames. These algorithms can provide real-time motion estimates and are computationally efficient. Additionally, feature tracking techniques or structure from motion (SFM) algorithms can be considered [14].

All algorithms mentioned prior create a 3D reconstruction of the scene, in other words, it is possible to see them as 3D scanners, the shape of the body is known, and orientation according to it can be calculated.

It is necessary to build a 3D scanner that works in real-time. This problem is known from mobile robotics applications and it is called SLAM - simultaneous localization and mapping.

SLAM can be solved by using several techniques for mobile robots. Multiple different sensors can be used but these devices are bigger and allow to use LiDARs and several cameras. To solve our problem it is possible to just use small and light sensors such as cameras. There are several methods of visual SLAM which can be used [15].

The list of SLAM algorithms:

- Lidar SLAM method
- Monocular ORB-SLAM method
- Monocular DPPTAM method
- Stereo SLAM method

2.3.2 Inertial measurement unit (IMU)

The second option can be inertial measurement units (IMUs) which incorporate a small IMU that consists of accelerometers and gyroscopes. The accelerometers measure linear accelerations, while the gyroscopes measure angular velocities. By integrating these measurements over time, the handheld device's motion can be estimated. Sensor fusion techniques, such as Kalman filtering or complementary filtering, can be applied to combine the data from the IMU with the visual-based motion estimates. This fusion helps to mitigate the drift issues associated with IMUs and enhances the overall accuracy of the motion estimation [16].

By combining visual-based motion estimation and IMU data through sensor fusion, you can take advantage of the strengths of both approaches. The visual-based estimation can provide accurate short-term motion information, while the IMU helps to maintain long-term stability and compensate for any visual tracking errors or occlusion situations. This combination is often used in applications such as augmented reality, indoor navigation, and gesture recognition on small handheld devices [17].

2.3.3 Other methods

Other options are machine-learning-based methods. These machine-learning techniques can be used to estimate motion by training models on large datasets. For example, recurrent neural networks (RNNs) or convolutional neural networks (CNNs) can process sequential data, such as sensor readings, to predict future motion based on historical observations [18].

2.4 Data visualization

It is possible to measure treatment parameters precisely, but when a handheld device is considered, the only person who can react and correct the parameters is the surgeon. That is the reason why visualization systems have to be designed. The goal of such a system is to show measured parameters in an intelligible way.

Most of the visualization during surgeries is done using screens. For example, a flexible tube (catheter) can be guided through a blood vessel to the heart to diagnose or treat certain heart conditions, such as clogged arteries or irregular heartbeats [19].

The data needed to be visualized in our case is much simpler. It is possible to show data by using LED diodes for example distance data. But it is important to not distract surgeons during surgery by the emitted light.

Another option can be projecting some parameters on the wound. The projection has been tested and figure 2.6 shows the results. For that kind of visualization, it is important to ensure correct contrast between light and black, which can be a bit tricky because the lights in operating room are strong [20].

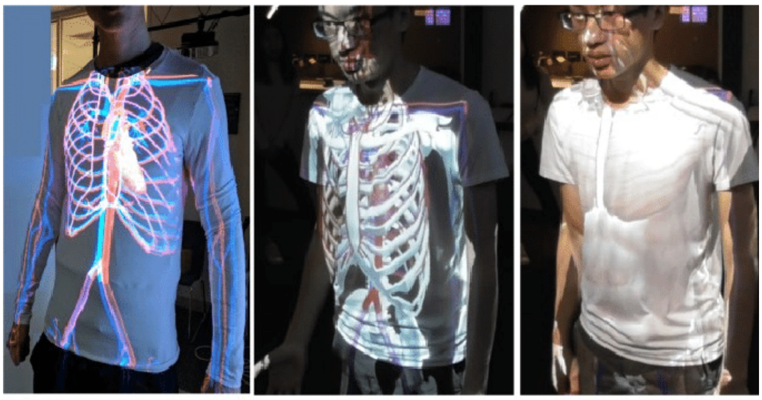

Figure 2.6. Projection on the body [20]

2.5 Linear stages

A linear stage, also known as a translation stage or linear motion stage, is a mechanical device used to precisely move an object or a load along a linear path. It is commonly used in various applications, including industrial automation, scientific research, microscopy, semiconductor manufacturing, and precision positioning systems.

The linear stages can help with dosing medication for patients. It is often called a syringe pump. The nurse inserts a full syringe into the device, adjusts the range, sets the speed of distribution and a precise motor will take care of dosing.

Figure 2.7 shows the syringe pump which is used for dozing medication, vitamins or nutrients into the patient in hospitals. Figure 2.8 shows the mechanical principle of such a stage and was inspiration for the first prototype linear stage [21].

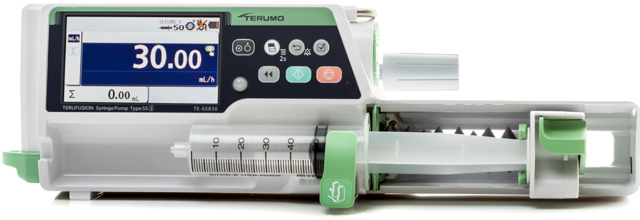

Figure 2.7. Syringe pump used in hospitals [22]

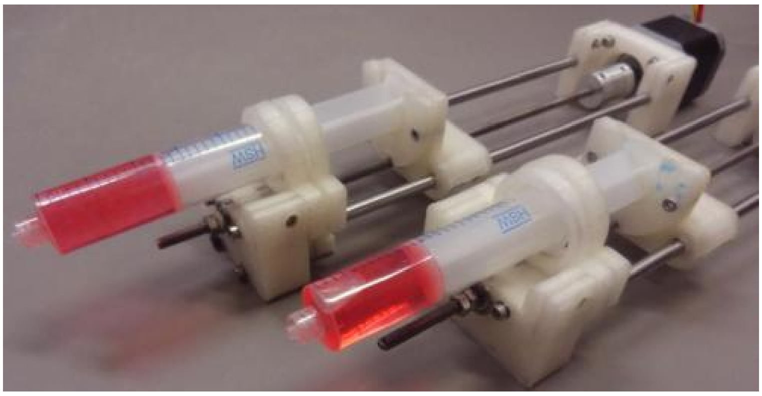

Figure 2.8. Mechanical structure of syringe pump [21]

Chapter 3
Measurement methods

3.1 Distance measuring

Distance measuring is a common type of measurement, everybody has at least once in their life needed to measure the length of some object, so they probably used a measuring tape or perhaps a ruler. Many methods have been developed, but their use cases vary depending on the measured distance. For example, it's not efficient to measure the distance between two cities by using the ordinary tape measure, instead data from GPS serves a better purpose.

In the project, the distance between the sprayer and the body is going to be essential, as keeping it 30 cm away is one of the main requirements for treatment testing phase, and it can vary in the future. From now on, let's consider distances **ranging from 1cm to 1m with precision of 1-10mm**. In addition to the range we have to keep in mind that it is not possible to touch the body wound during the measuring, therefore it is necessary to **consider only contactless measurement methods**.

Distance measurement can be divided into two groups. Firstly, we have direct measurement which is for example using the tape. During the process, we set the tape and read the value from the end of the measured object. On the other hand, there are indirect methods when another parameter is measured and the distance has to be calculated. All methods discussed in the following sections are **indirect methods**. The conditions of our measurements are quite precise, so let's discuss the available measuring methods which can be used and were used in different projects.

3.1.1 Transit-time measurement

This form of measurement is based on receiving a reflected signal as well as measuring the time in between transmitting the signal. When we know the time it takes for a signal to reflect, it is simple to calculate the distance. The main concept is depicted in the time of flight sensor (ToF) in figure 3.1.

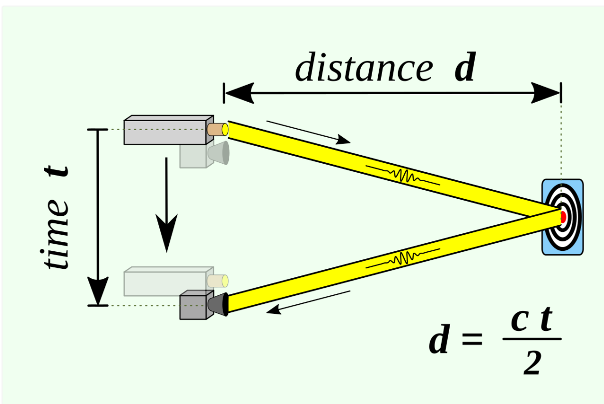

Figure 3.1. Principle of Transit-time measurement [23]

There are several conditions on which the measurement highly depends, the most important factors are the type of signal and speed of propagation. For example, such a signal could be light or sound. The speed of propagation also depends on the environment (density, temperature, humidity, ...) there are different speeds of light in vacuum and water. Another factor is the reflection of the signal on the object's surface. The reflection depends on the shape, texture, and size of the object and also the angle between the transmitted signal and the object.

Here is a list of factors that influence the transit-time measurement:

- type of the signal
- environment conditions
- signal reflection
- shape, texture, size of the object
- angle of impact

The distance in specific conditions can be calculated by using equation (1). The equation assumes that the reflection is considered to be perfect, which is valid when we are considering a human body as a reflective material. The reflection is perfect when the angle between the signal and the body is perpendicular.

$$d = \frac{ct}{2} \tag{1}$$

Where d is the distance between the source of the signal and the reflection object $[m]$, c is the speed of signal (sound or light) $[m/s]$, and t is the time in between transmitting and receiving the signal. It is important to mention that this equation is valid when the transmitter and receiver are relatively close to each other.

List of transit-time sensors:

- Time of flight (ToF) sensor
- Ultrasonic sensor
- Radar sensor

3.1.2 Camera based methods

Camera methods are a strong tool for the extraction of data from the real world. These methods highly depend on the image recognition and quality of the camera. Cameras have several parameters such as frame rate, resolution, and field of view which are important to address for choosing the correct image recognition method. Most of the methods start with feature detection, there are several techniques on how to achieve it. This detection should provide the positions of the features in the image coordination system, the units are pixels. After they are detected, we can use several methods to process the data, depending on what our desired outcome is. For instance, we use a different method if we measure distance and if we measure speed.

It is possible to use laser pointers to detect distance in between source of the light, which is fixed to the camera, and projection plane - in our case body of the patient [24]. In a real scenario, the laser pointers are fixed in parallel with the center axis of the camera.

This distance estimation uses the pin hole camera model, which reduces the complexity of a camera to a very simple model, as shown in figure 3.2. The way to imagine how this model works is to imagine a box, which has a detection plane on one side and a small hole through which light passes on the other side. Calculating distance by using it is thereby very straightforward. Equation (2) is used to do so, and because the focal length (fy) and distance between the center of the camera and laser pointer (dY) are a fixed value, the distance (dZ) only depends on an easily measurable factor - the distance in the image coordination system (dy). We can use the pinhole camera model, as image processing algorithms can change the image frame after calibration.

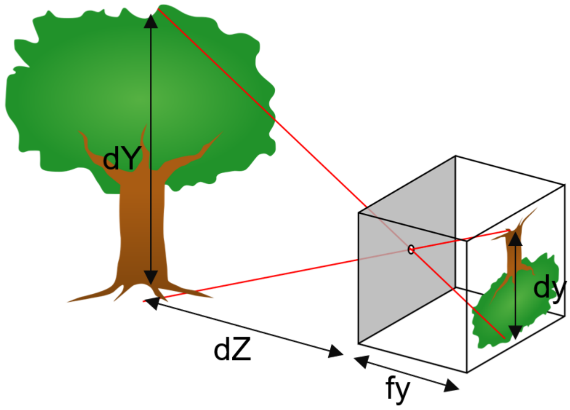

Figure 3.2. Pin hole camera model

$$f_x = \frac{d_x}{d_X} dZ \tag{2}$$

$$f_y = \frac{d_t}{d_Y} dZ$$

Where fy is the focal length of the camera in y direction $[cm]$, dy is distance in the image coordination system $[pixels]$, dY is the distance in the real-world coordination system $[cm]$ and dZ is the distance in between camera and projection plane $[cm]$. The same equation works for X axis.

The calibration of the camera is an important step for this distance detection method, the same as it is for all other camera based methods. However, for this method in particular, it is necessary to know the focal length of the camera, which is one of the result parameters of the calibration.

3.2 Speed detection

The speed at which the sprayer device moves during the procedure is yet another important parameter. There is no direct method of speed detection on the market, so all measuring methods are indirect, which means that the speed is calculated by using different values.

A great example of such a value is the position or acceleration, and there are known relation in between them (3), and when we measure one value it is not hard to derive the rest. The following two subsections describe the measurement techniques based on acceleration and position, which are possible to use in our case.

$$a = \frac{dv}{dt} = \frac{d^2x}{dt^2} \tag{3}$$

Where a is acceleration $[m/s^2]$, v is speed $[m/s]$ and x is position $[m]$.

The movement speed should be 3 cm/s which is quite slow meaning surgeons could struggle with keeping it. Same as for distance detection, the sensor for movement speed detection will be placed in a hand-held device and also can be different in the final application.

According to figure 5.2 our goal is to measure movement speeds in X and Y axes, in other words in a plane that is parallel to the body surface. For testing purposes, it is possible to make the simplification that the body is just a plane, which would work for example for large back burns. In real cases, the movement speed have to be result of summation the movement speeds in individual axes (X,Y,Z).

3.2.1 Method based on IMU

IMU stands for inertial measurement unit and this method measures acceleration, angular rate, and earth gravity. Said data, especially acceleration, helps us calculate movement speed. It is calculated by the integration of acceleration (4).

$$\vec{v} = \int \vec{a}\ dt \tag{4}$$

Where $\vec{a}$ is acceleration, and $\vec{v}$ is speed.

The acceleration is measured in 3 axes (X, Y, and Z), the IMU also measures earth gravity. For example, when the IMU has the Z axis perpendicular to the ground, the earth's gravity will be present only in the Z axis. The other axes will be zero when there is no movement. In this scenario, it is possible to extract the gravity just from the Z axis and the speed in each axis can be calculated by using the equation above (4). But this edge case is impossible to achieve in a real scenario as the IMU is at least slightly tilted and the earth's gravity is not zero in other axes. That is the reason why it is necessary to also measure the orientation of the IMU against the ground. When we know the precise orientation of the IMU, the speed can be calculated according to the equation below (5).

$$\vec{v} = \int \vec{a} - 10\vec{\sigma}\ dt \tag{5}$$

Where $\vec{a}$ is acceleration, $\vec{v}$ is speed, and $\vec{\sigma}$ is orientation in range [0-1].

No measurement is precise in real cases, and for that reason, fusion algorithms were introduced. These algorithms combine measured data from all sensors in the IMU and output speed and position as an output. Great example such fusion algorithm based on Madgwick's PhD thesis [25] with open-source code available on git-hub [26].

3.2.2 Triangulation method

Triangulation is used for example for tracking cell phones [27]. The location is calculated using the known location of cell towers and the strength of the signal. Besides, Bluetooth can be used for tracking [28]. Another application that could work as an inspiration for our project is VR headsets tracking.

One of the VR headset tracking techniques is based on base stations which are placed in the opposite corners of the play zone. These base stations emit laser beams with different coding and specific timing. The headset receives signals from both stations and calculates the time in between receiving signals from each base station in different axes and by triangulation the position is calculated. From the detected position of the player movement speed can be calculated (6) [29].

When we are considering a device that has two different parts. One is stationary with a computer inside and the second with a dispensing system and sensors as a handheld device. There would be the possibility to use some measuring system which is used for example for tracking VR kits, but the problem is when someone is standing in between a stationary part and a handheld device. But several different methods of tracking are used in different projects.

3.2.3 Camera method

The idea behind the camera based method is quite simple. Firstly, an algorithm finds some features in one image frame and saves their position. Afterward, it tries to find the same features in the next image frame. In the next step, it subtracts their position shift from the image frames. In this stage, the algorithm knows the distance traveled between the two frames in the image coordinate system (in pixels). After that, the distance is calculated in the world coordinate system, which uses the pinhole camera model. 3.2 It is necessary to use the measured distance for our calculation, based on equation (2).

The system precisely tracks the position of the sprayer during the process. In order to calculate speed the position is derived by the time. In this method, the position is divided by the time between the two image frames.

$$v_x = \frac{d_X}{dt} = \frac{\Delta X}{\Delta t} \tag{6}$$

Where v_x is movement speed in X axis $[m/s]$, ΔX is the distance traveled by sprayer in between two frames $[m]$, and Δt is time between two image frames.

For correct results filtration is necessary to use.

Camera based method in steps:

```
1. Find features in the first image frame
2. Find the same features in the next image frame
3. Calculate the distance between features in different frames
4. Change the coordinate system (image to world)
5. Calculate the speed from position
6. Filtration
```

This camera based method is inspired by several papers which use similar techniques for calculating the speed of vehicles from camera recording [30–31].

3.3 Orientation detection

It is important to control the orientation of the sprayer against the body wound as it influences the spread of the medication on the wound. In figure 3.3 it is possible to observe the difference between when the sprayer is perpendicular to the body wound and when it is tilted 45 degrees. The spread won't be uniform at all. So in most cases, our goal is to have the sprayer as perpendicular as possible to the body wound. It is important to mention, that in some cases especially at the edges of the body wound we have to tilt the sprayer.

The previous example was based on plane body wound estimation, but the real wounds are not plane. It is necessary to first estimate the shape of the body wound and based on that calculate the orientation of the sprayer. There are several methods on how to solve this issue. One solution can be based on sensors and rough shape estimation, another solution can use 3D scanning, it is not described in this section, because it is possible to estimate a 3D model of the body by using a depth camera 2.3.

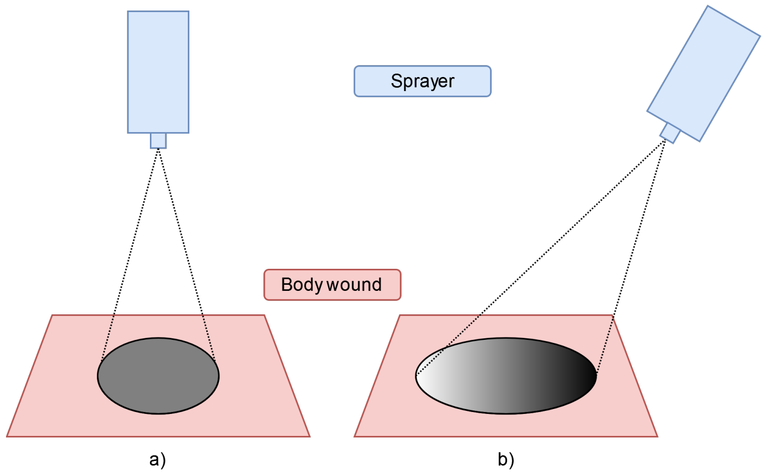

Figure 3.3. Medication distribution in different sprayer orientation a) The sprayer is perpendicular to the body wound b) The sprayer is tilted in 30 degrees against the body wound

3.3.1 Structured light

This method is based on projecting a specific light pattern (structured light) on the shape which we want to detect. A camera decodes the pattern and an algorithm estimates the shape. It is a lightweight and quite old method of 3D scanning. Said method was developed in the previous century [32] and was successfully used in several applications, for example, Xbox360 kinect sensor or for edge detection in welding processes [33].

This problematic is not new and several papers were published about it. One of them presents a robust, structured light for 3D reconstruction and the results are visible bellow 3.4 [34].

3.3.2 Time of flight sensors

For our solution, it is not necessary to use a computationally expensive 3D scanning method. It is possible to measure the distance between the sprayer and the body just by using the spray profile of the nozzle. One dimension is necessary to measure the distance in the center of the spray profile and on its edges, so three distance sensors for one dimension can be sufficient. For both dimensions, five sensors could be sufficient 3.5.

3.3.3 LiDAR

The time of flight sensor method is very cheap, but it struggles with ToF sensors. Their field of view can be around 15 degrees, from a distance of 30 cm it can only measure distance in an area of $8x8\ cm = 64\ cm^2$ and we do not know where exactly. A solution to this issue can be to use ToF sensors with a small field of view.

LiDAR (Light detection and ranging) is a system that works on the same principle as ToF sensors. However, it uses a laser source of light that has a field of vision equal to almost zero, and a mirror system is used for changing the direction of the laser beam. Figure 3.6 shows the principle of LiDAR.

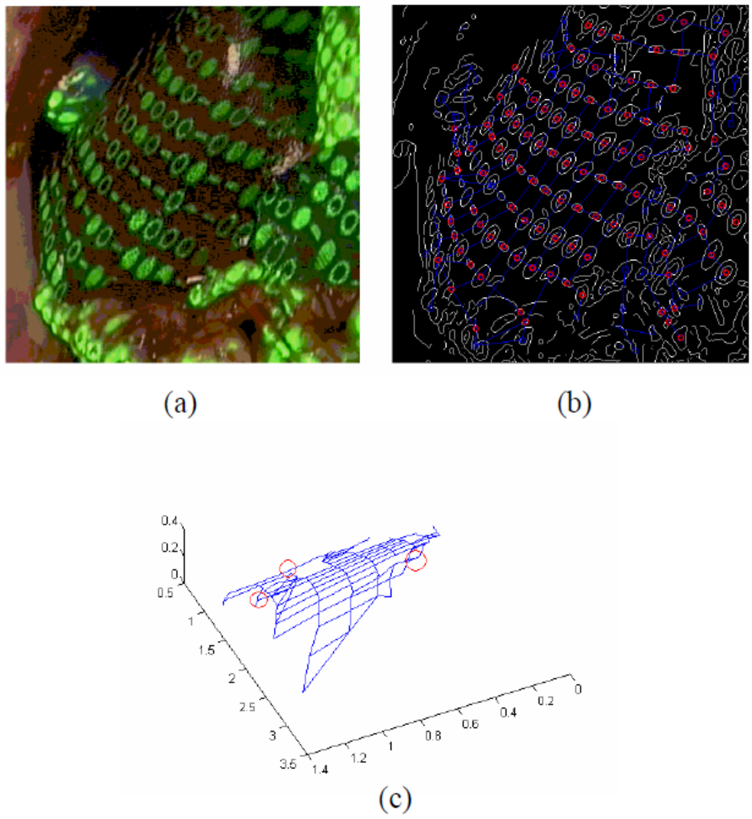

Figure 3.4. Example of structured light a) The projection onto internal structures of a pig abdomen with additional white light b) Detection and decoding c) The projective reconstruction [34]

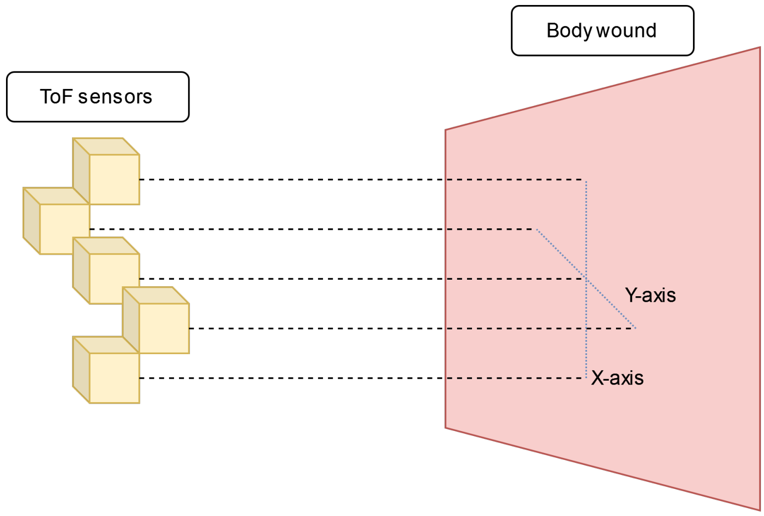

Figure 3.5. Time of Flight matrix for orientation measurement

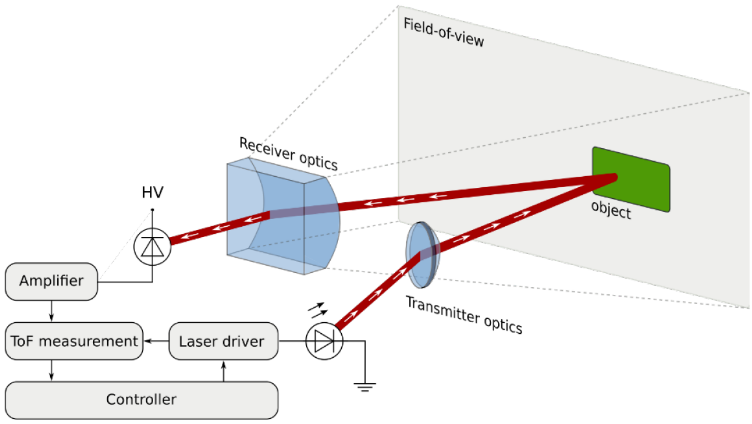

Figure 3.6. LiDAR principle [35]

Chapter 4
Method validation

As was described in the theory chapter, there are several methods how to measure different properties, this chapter describes tests that have been done and helped me to understand the advantages and disadvantages of individual methods. With this knowledge, it was possible to choose the correct methods for prototypes.

Most of the validation was done by using prototype zero or specially designed components that could be used in the prototype.

4.1 Distance measuring

List of distance measuring methods/sensors which can be used in the project and were tested:

- Two parallel laser beams and camera detection
- Aruco markers with camera evaluation
- Time of flight sensor
- Ultrasonic sensor

These measuring methods have been chosen because of their limits, range, and size.

4.1.1 Aruco markers

Aruco markers are a special image type widely used in image detection. They are in certain ways similar to QR codes, and algorithms are ready for detection, same as QR codes they can code some information. Different IDs were used in our case.

The first experiment tested if Aruco markers can be used as a reference for other methods. The standard deviation of measuring error was 0.07 cm. I decided to use the Aruco markers as a reference for other distance-measuring methods. The average measuring error of -0.66 cm was subtracted for future use. Real distance was measured by using a ruler. A webcam was used for capturing and evaluation was done on a normal laptop by using OpenCV. The setup, Aruco marker, and its detection are shown in figure 4.1.

It is important to note that this method can not be used in our prototype because it would be very hard to place the markers on the wounded body's surface during surgery. This method is mainly used for future distance and speed-measuring tests.

4.1.2 Two parallel laser beams

The principle of measuring distance by using two parallel laser beams is described in theory chapter 3.1.2.

Before the laser dot detection procedure, it is important to prepare the camera for it. It is important to get rid of distortion and set the correct focal length (fx) of the camera.

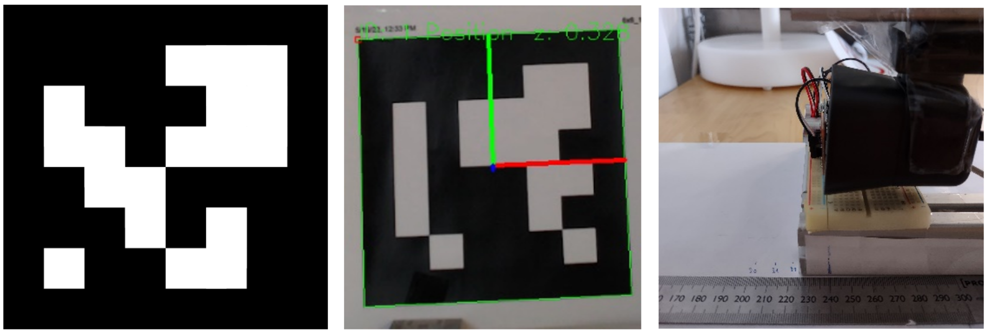

Figure 4.1. Aruco marker, its detection and setup for validation test

The distortion was calculated by procedure described by openCV [36]. First of all, it is necessary to take a few pictures of printed chessboard (56 in our case) and afterward, several functions is used:

```
cv2.cvtColor()
cv2.findChessboardCorners()
cv2.cornerSubPix()
cv2.calibrateCamera()
cv2.getOptimalNewCameraMatrix()
```

The focal length set has been done automatically by using Aruco markers. The result of focal length determination together with laser dot detection are visible in figure 4.2.

Laser points detection is done by openCV library and functions listed below are used:

```
cv2.threshold()
cv2.findContours()
cv2.minEnclosingCircle()
```

When the position of all dots in camera frame are known algorithm sorts them and choose the two closest to the center point. The results are shown in figure 4.4 where all distance methods are compared.

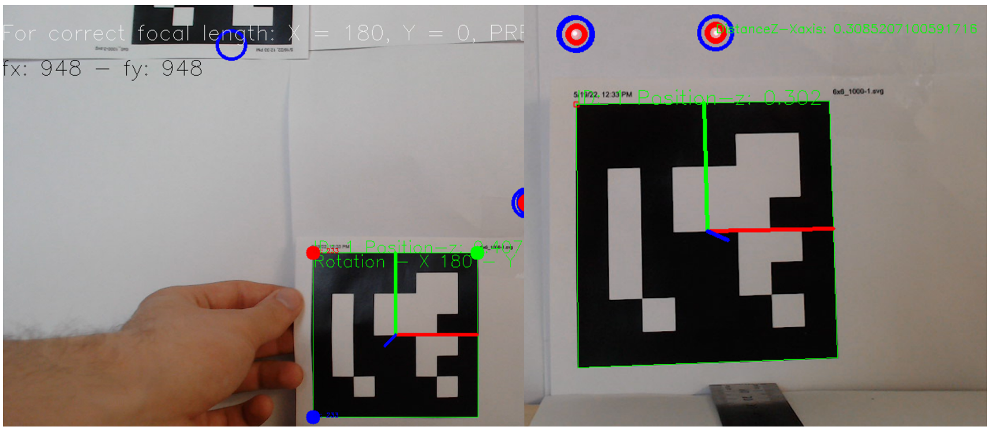

Figure 4.2. Set of the focal length, and laser dot detection

This method has several disadvantages:

The quality of results is highly dependent on laser dot detection. Even more so when we are considering detecting laser dots on a wounded body in an operating room. There are very bright lights meaning the detection could be inaccurate.

The detection works precisely only when the camera and laser beams are perpendicular to the surface. Otherwise, there is a measuring error that increases with a tilted angle. Detection depends on the quality of the used hardware, a small refresh frequency can be used when we are considering an embedded solution. Alternatively, it is possible to rewrite and optimize the detection algorithm for embedded solutions.

The main advantage of this method is the identifiable location and visibility of laser points. These points are used in distance calculation and help the surgeon determine the distance to an exact point with the laser light.

Sensor methods are the exact opposite, they do not show/point to the exact point of the measured distance.

4.1.3 Ultrasonic Sensor

The sensor uses a sound pulse and measures the time between sending and receiving the pulse, described in 3.1.1. For testing, the HC-SR04 ultrasonic sensor was used. The main disadvantage is the big field of view of the sensor and the unknown reflection point. In other words, we do not know where the distance is measured.

On the other hand, this sensor does not require any lighting conditions, which is beneficial because of the lighting problems in operating rooms.

The comparison with other methods is shown in figure 4.4.

4.1.4 Time of flight sensor

This sensor works similarly to the ultrasonic sensor, with the difference that it uses a light signal instead of a sound signal. The sensor has a smaller field of view than the ultrasonic sensor.

Two different time of flight sensors were available for testing.

The first one is VL53L1X, with field of view $15 - 27°$ and a distance of 30 cm in between sprayer and surface. Meaning that maximal area of detection is 15x15 cm. For comparison, the ultrasound sensor has a field of view smaller than 15° which measures distance in area 8x8 cm. This sensor has one sensor and one receiver. The results are also showed in figure 4.4.

The second sensor TMF8821 was not tested and has one main difference. It has a matrix of receivers which enables us to get an estimate of the shape of the observed surface. In our case, it could work as an angle detector and also as a distance sensor.

Another experiment was done for the ToF sensor. I was comparing the measurement results between water droplets in between the sensors and when no droplets were used, just air. Results showed that there is no difference between these two cases, figure 4.3.

4.1.5 Comparison of distance measuring methods

A comparison of all distance measuring methods is shown in table 4.1 and figure 4.4. Another table 4.2, shows the difference between the measured and real value (error value). Real distance is the distance measured by using Aruco markers. The most important parameter is the standard deviation of the error value. And because the two parallel lasers method has the smallest standard deviation error 0.45 cm, it is the best method for detection distance. The ultrasound method also looks promising as it is independent from light.

4.1.6 Curved surface test

A flat reflection material has been used for previous tests. In reality, the distance is measured between the sprayer and the body, not said reflection material. Every part

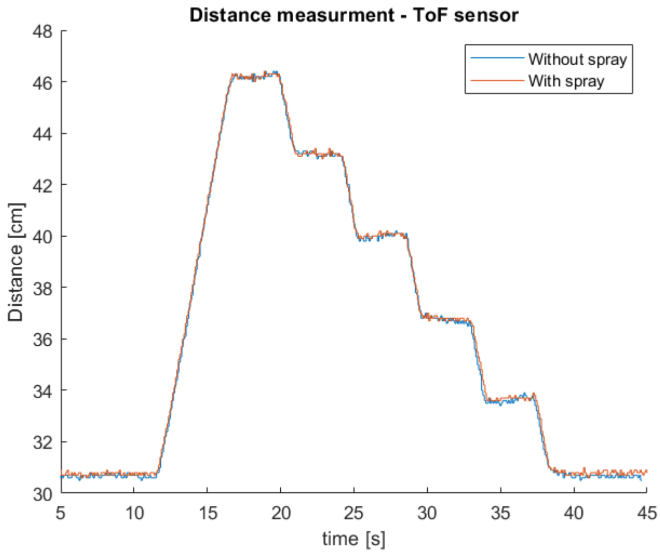

Figure 4.3. Comparison ToF distance measurement with and without spraying

Real distance [cm]	Laser[cm]	Ultrasound [cm]	ToF [cm]
24.3	23.9	23.5	23.0
27.1	26.5	25.5	25.9
28.9	28.6	26.7	28.5
30.1	30.8	27.6	29.5
31.0	31.0	28.6	30.5
34.0	34.0	31.5	33.8
37.1	37.0	35.7	37.7
40.0	39.2	37.8	40.0

Table 4.1. Distance measurement methods comparison

Real distance [cm]	Laser[cm]	Ultrasound [cm]	ToF [cm]
24.3	0.4	0.8	1.3
27.1	0.6	1.6	1.2
28.9	0.3	2.2	0.4
30.1	-0.7	2.5	0.6
31.0	0	2.4	0.5
34.0	0	2.5	0.2
37.1	0.1	2.4	-0.6
40.0	0.8	2.16	0
Average	0.1875	2.07	0.45
Standard deviation	0.458	0.591	0.619

Table 4.2. Error value comparison of distance measurement methods

of the body is curved differently. The radius of the curvature can vary from small such as back to big like an arm.

Additionally, different surfaces should be considered, it was not possible to test the reflection properties of a body wound, but it is possible to use a surface that has a similar texture.

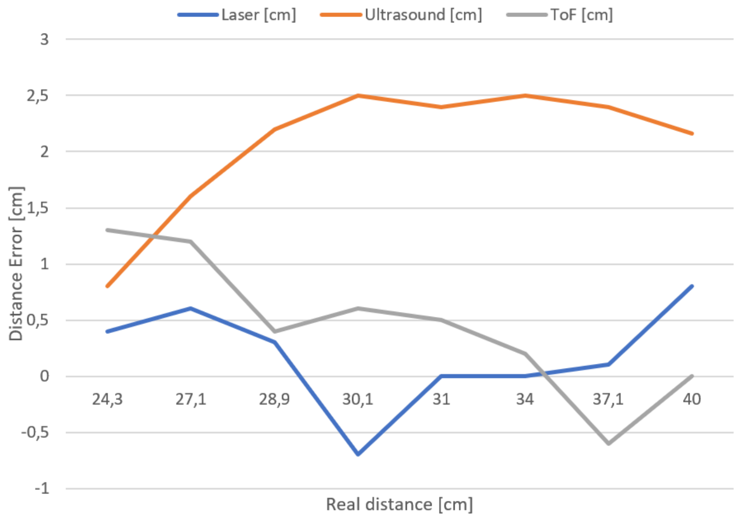

Figure 4.4. Distance methods ERROR comparison

Following figure 4.5 which shows the experimental setup, a precision linear stage was used to move in X-axis. Distance (Z-axis) is measured by the Time of Flight sensor, and ultrasound. Aruco markers are used as a baseline, the markers are placed 15 cm next to each other. Firstly, distance without any obstacles was measured 4.6. A pillow is used in the next test, results in 4.7 show that the ultrasound has a problem with detecting the edge of the pillow. Thereby, it is possible to conclude that the ultrasound sensor has a problem detecting curved surfaces.

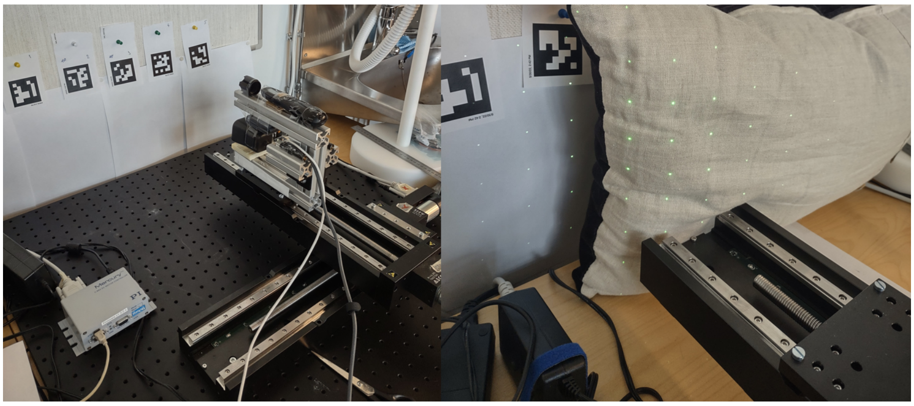

Figure 4.5. Distance measurement - cured surface, setup

4.2 Speed detection

Principle of the speed detection method are describes in theory section 3.2.

For several tests, precision linear stages made by Physik Instrumente were used. The stages are shown in figure 4.5. And require specialized controllers which are connected to the computer via USB.

4.2.1 Camera method

In this method, the idea is simple, let's find some features in one image frame, save their positions, and try to find the same features in the next image frame. Then, subtract

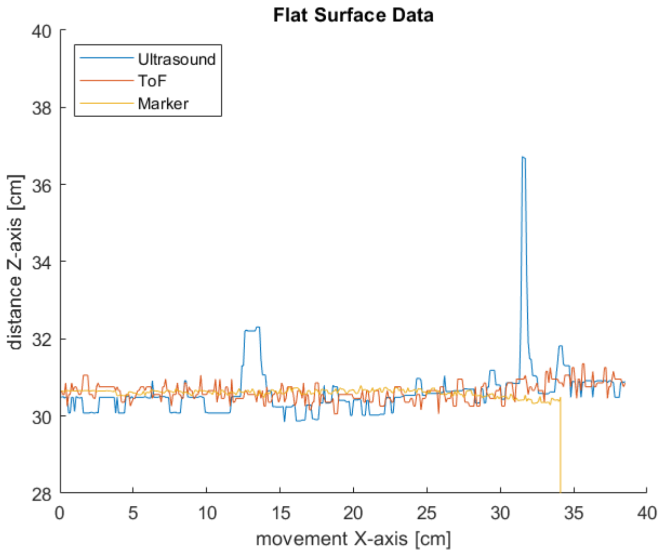

Figure 4.6. Distance measurement - flat surface

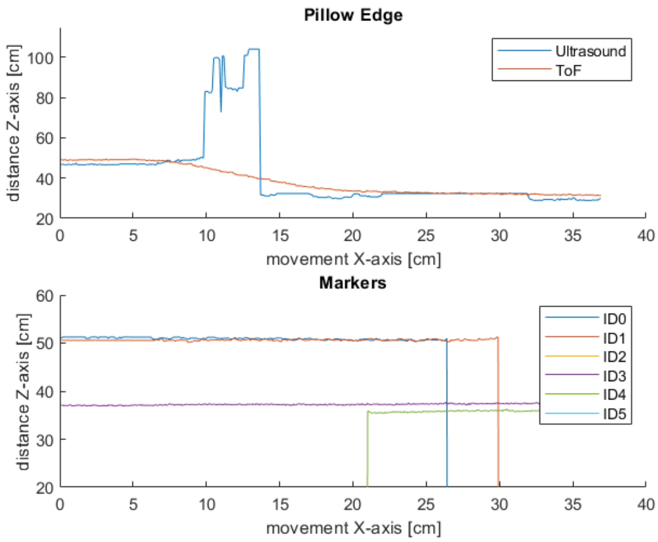

Figure 4.7. Distance measurement - curved surface

the positions of the features in different frames, and with the measured distance in Z-direction we can calculate the differences between every position of the features in a global frame. When we divide these position differences by time in between frames we calculate movement speed.

Firstly I tried to use the positions of Aruco markers in between individual frames for speed estimation. Precise linear stages were used for validating.

In the first experiment, I set up velocity of linear stage movement. It was 0.02 m/s, 0.03 m/s, 0.025 m/s, and 0.04 m/s, this movement profile is visible in figure 4.8. Than I compared the movement profile with the calculated movement profile from the positions of Aruco markers. The calculated movement speed is visible in figure 4.9. And table 4.3 shows the means and standard deviation (std) during movements.

The calculation is described in theory section but in short it is just derivation during time. Additionally, simple window filtering have been done in figure 4.9.

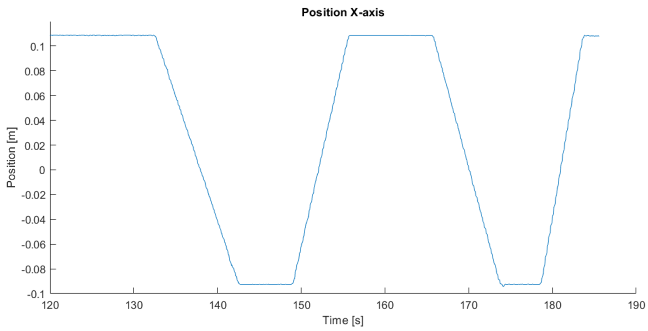

Figure 4.8. Movement profile for camera speed detection test

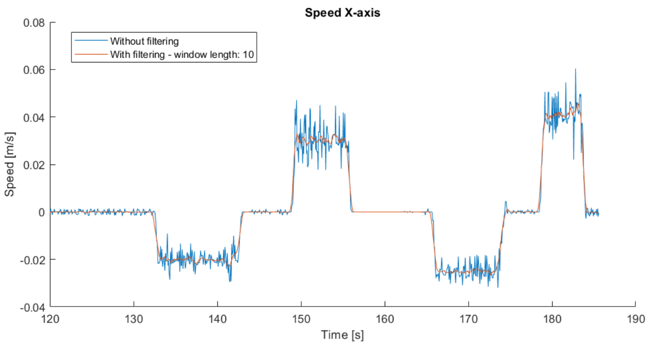

Figure 4.9. Movement speed calculated from positons of Aruco markers

Real distance [cm]		0.02	0.03	0.025	0.04
Measured Speed	Mean	0.0202	0.0304	0.0251	0.0414
[m/s]	Std	0.0035	0.0062	0.0033	0.0063

Table 4.3. Comparison of real and measured speed for Aruco markers

Because the experiments with Aruco markers looked promising and the speed estimation was quite good. I decide to try experiments with feature tracking. OpenCV library was used, more specifically these functions:

```
cv2.ORB\_create
cv2.flannBasedMatcher
cv2.findHomography
cv2.perspectiveTransform
```

As of yet, no proper comparisons have been done. I decided to not rely on the camera method based on feature tracking. Mainly because of the difficult light conditions in operating rooms and the hard-to-track features in open wound images. Also long computation time was problem - two frames per second on the first prototype. However, it could be possible to use another method of finding features than the methods which openCV offers, probably use some machine learning methods.

4.2.2 Sensor method

The camera based method is trying to deal with the derivation of position to calculate speed. And the sensor-based method uses an inertial measurement unit (IMU) which measures acceleration, angular rate, and earth gravity, from this data, especially from acceleration which is integrated in order to get a movement speed. This method struggles with drift. Meaning the acceleration not being zero when it should be zero, in most cases it is cheap sensors that suffer from this kind of problem. More about IMU is possible to read in theory 3.2.

I tried to calculate speed during linear movement. I measured acceleration data in a stable position and afterward during the movement. In order to get rid of drift I subtracted the mean of acceleration data in a stable position from the acceleration data during movement. The result looks quite promising and the visualization is shown in figure 4.10.

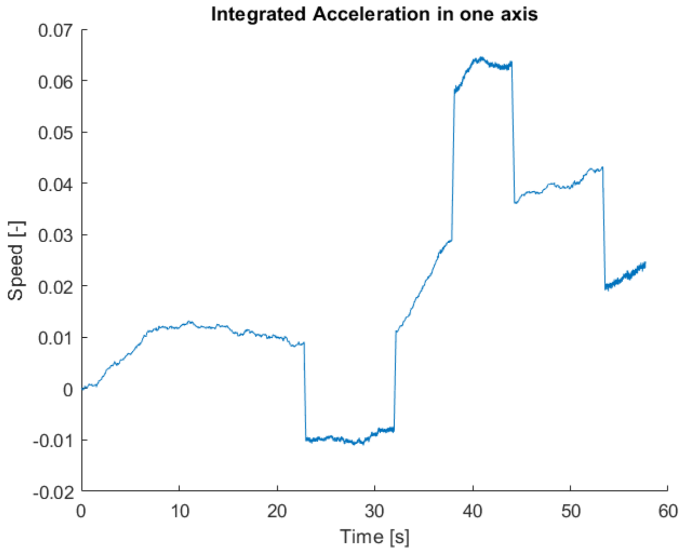

Figure 4.10. Speed detection by using IMU

But this approach is not possible to use in practice, because here just one position is used. Yet in reality, it is necessary to always subtract earth gravity and determination of the earth gravity vector is not easy and it has some errors.

Afterward Fusion algorithms were founded, this one is the best one which was tested: [37] https://github.com/xioTechnologies/Oscillatory-Motion-Tracking-With-x-IMU/blob/master/Script.m

For all test the accelerometer calibration have also been done.

4.3 Orientation detection

This problem is related with estimating shape of surface, eventually with 3D scanning. Figure 4.5 shows projected laser dots on pillow and with processing 3D estimation can be done.

Only structured light was tested. Think for example laser grids, because this grid will change when the shape of the surface will be uneven. Unfortunately, this method can not be used for estimation orientation because the camera sees the structure light in the same position even when the surface is not perpendicular to the camera and structure light source.

Chapter 5
Design and implementation

5.1 Prototype objectives

Before diving deep into the description of individual solutions, it is important to define key requirements. These requirements are essential for maintaining the correct treatment properties of applying and describing the current technology used.

In a nutshell, during the surgery and the process of applying, it is important to stick with these conditions:

- Keep the distance between the sprayer and the wound at 30 cm
- Apply the medication uniformly on the wound

To achieve the uniform distribution it important to:

- Have the nozzle as perpendicular as possible to the body wound
- Keep the same speed of movement of the sprayer, roughly 3 cm/s
- Apply the same amount of medication during the time of surgery

5.1.1 Current solution

Currently, the spraying procedure is done by surgeon, the hardest part is to maintain all of the requirements listed above. An image that was taken during applying process shows the sprayer Baxter EasySpray 5.1. This device has two syringes with Tisseel® fibrin sealant and cells. These two syringes are connected by a nozzle which ensures the circular spraying profile. The nozzle also has an input for pressured air. The surgeon can then control the amount of medication and glue applied while spraying, but the spraying itself is done by pressured air.

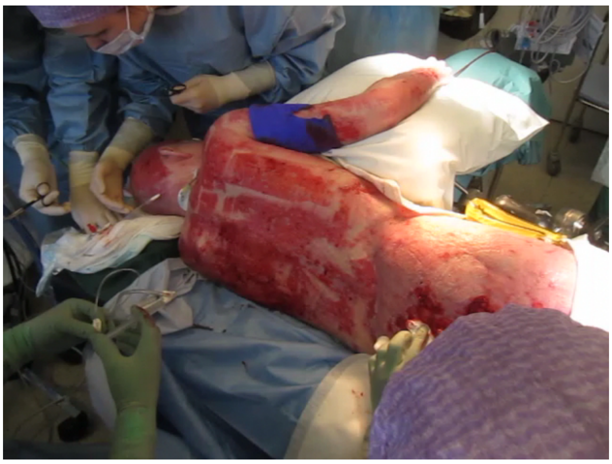

Figure 5.1. Current applying procedure

5.1.2 Proposed solution

The spraying has a strong potential to be automatized, but first of all, it is necessary to define specific goals and conditions which the automation will try to achieve.

One way how to deal with the problem would be to design a device from scratch which would be fully automatized. An example of such a solution could be to use a 6-axis manipulator with a special end-tool. However, it would be challenging to pass the surgeon's knowledge to the computer, and of course, it would require a lot of work. Perhaps the biggest hurdle of all would be the price of such a device. The device's cost would be so high that the burn center would prefer to use the old types of healing and overall cheaper technology. Mainly because our method would not be paid back during its lifespan and the level of treatment would not be significantly higher.

Another solution for maintaining all of the requirements is to construct a device that does not fully provide an automatized solution. Instead, it works as a helper to the surgeons during the surgery. The solution is a hand-robotic device that measures the essential data, shows them to the surgeon and he/she can use this information to adjust the spraying procedure.

The device will be inspired by the current solution and use basically the same device Baxter EasySpray. The reason for this is that said method is fully certified and it is easier to use a device that can be used in practice right now, even though it is necessary to adjust a few things to the current solution. However, after the new method will be proved we can change the design and use a new approach in the core parts of the application.

This information is important to keep in mind when we want to design the proper device:

The goal of this project is to design and build a device that helps surgeons with applying cell-based medication for burned patients.

The main purpose of the device is ensuring repeatability of the new treatment method or at least made the repeatability more reliable.

The proposed system is a hand-robotic device that applies cell-based medication and ensures its uniform distribution on the burn wound. The hand-robotic device measures the distance between the sprayer and the wound surface. It detects the shape of the treated body part around the wound, measures how the sprayer is rotated in relation to the wound, and measures the speed of movement of the sprayer against the damaged tissue in the horizontal direction. The system uses a signaling system to navigate the surgeon to ensure a uniform distribution of the cell-based medication.

For correct medication distribution, the sprayer must be 30 cm away from the body. The sprayer also has to be as perpendicular to the burn wound as possible, even though the body's shape is not flat. And the speed in the horizontal direction must be 3 cm/s 5.2.

Additionally, an algorithm for controlling the uniform distribution of medication can be developed. In other words, the device knows how thick the layer of medication is applied on the surface of the burned wound, and it can predict, based on the shape of the body, the best movement trajectory.

Another way how to deal with the problem could be to use a fluorescent substance and add it into the sprayed liquid. Afterward, the surgeon could see where was the medication applied.

Problems to solve:

- Measuring the distance between the sprayer and the wound
- Measuring movement speed

- Orientation detection
- Dispensing system
- Signaling system

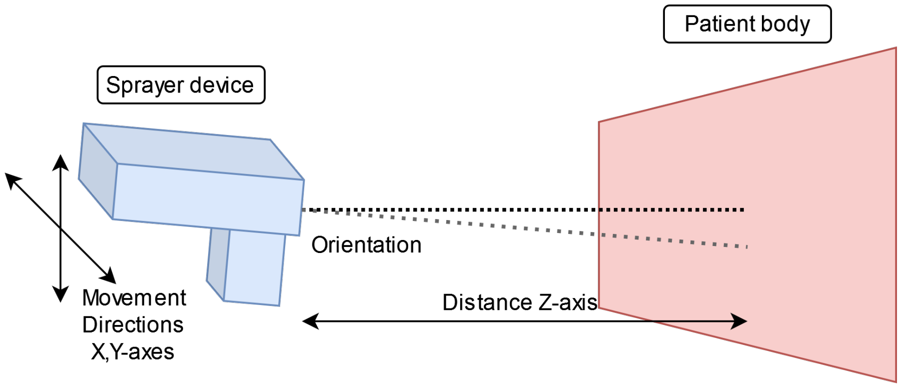

Figure 5.2. Device with all problems to solve

5.2 The first prototype

The first prototype 5.3 was built to prove that it is possible to construct a device that helps surgeons during surgery and provides some basic feedback. However, it was not determined for use in practice, because the sanitation norms were not known. Also, surgeons could get a rough idea of what they could use in practice and their comments are mentioned below 6.1.1, and it was constructed as a prove of concept.

It measures the distance between the sprayer and the surface, it also contains a dispensing system. Three buttons are used for controlling the prototype. Five LED small diodes and one power LED indicate the distance from the surface. The prototype also contains Raspberry Pi Camera V2 which streams the video to the screen. Except for the power source, all HW is placed in the hand-held device.

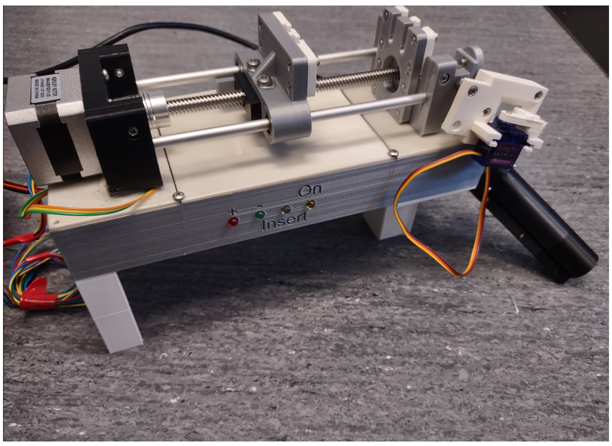

Figure 5.3. The first prototype

Time of flight sensor is used for distance measuring in the first prototype, based on validation sections 4.1.5 and 4.1.6 it has the best performance for embedded solution. The results are satisfactory. Measuring speed is not implemented in the first prototype. The software is running on Raspberry Pi 4, inputs and outputs are connected using a

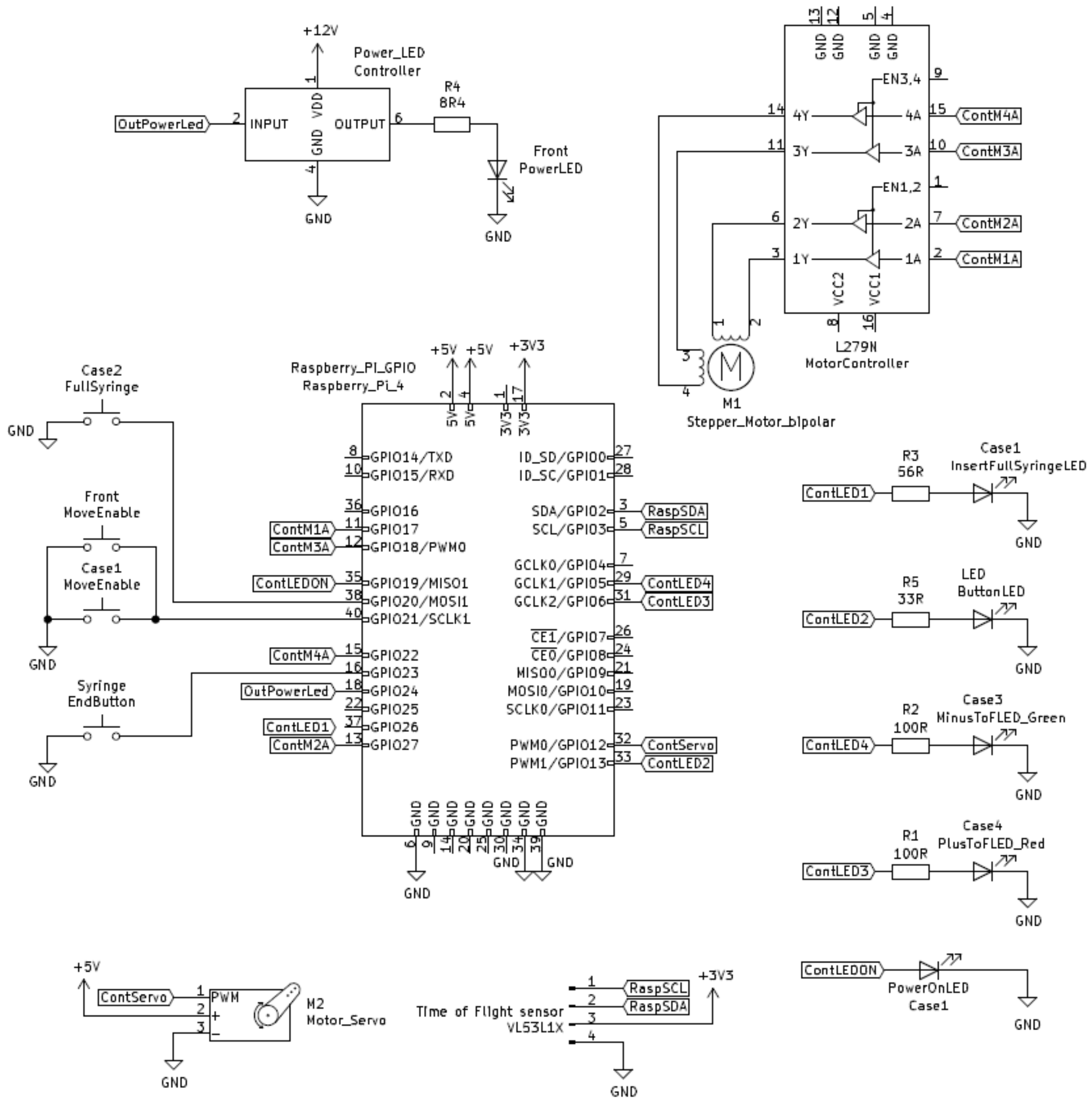

Figure 5.4. Circuit diagram of the first prototype

breadboard to the GPIO pins of the Raspberry. Breadboard was used because of time pressure but the circuit diagram was created 5.4 and it would not be a problem to make PCB.

5.2.1 Linear stage

The main part of the linear stage is inspired by open-source syringe design [21]. It contains a stepper motor that rotates a screw rod. The rod linearly moves the end of the syringes. Two different screw rods were used for testing. The first one is with a classical metric thread M5 and the second one is with a thread that is used for linear motors and 3D printers Trapezoidal ACME-8. The main difference between rods is that the metric rod moves the linear stage for 0.8 mm per turn and the trapezoidal rod moves the linear stage for 8 mm per turn.

The metric thread is the better choice for very slow moves. The move with the same speed by using the ACME thread is noisy and shaky but a better stepper controller with more microsteps could solve the problem. For fast moves, for example returning to the initial position, is much better to use the ACME thread. The rod that will be used in real surgery or in the next prototypes depends mainly on the applying speed, but in this development stage, the goal is to have the device universal and for all types of syringes and all kinds of dispensing speeds.

The second part of the linear stage controls airflow 5.5. Because of the easy integration of the device into the medical environment, the current control air system is used, this system uses a button that enables the surgeons to control the airflow. Said air button has just two states, on and off, it is basically the Baxter EasySpray shown and described here 2.2.4.

The servo is placed in a custom 3D printed case and it manually controls the air button in the same way as a surgeon would.

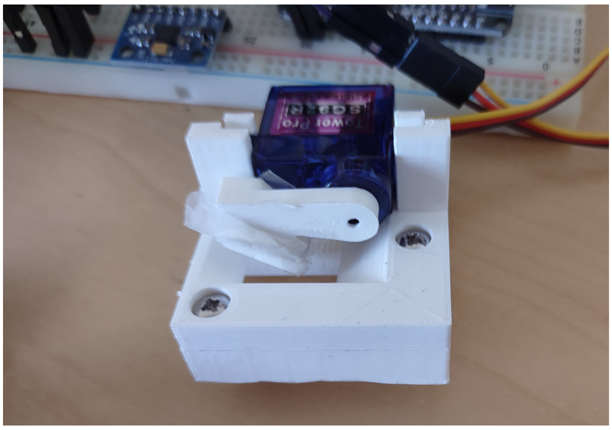

Figure 5.5. Airflow control

The end button is used for calibration because when the device is without power anyone could rotate the thread. Meaning it is safer to find the zero position whenever the device is turned on and not rely on the zero position from previous use.

List of components used for linear stage:

Electronics:

- Raspberry Pi 4 B 8Gb
- Stepper motor – ROB-09238
- Stepper motor driver – L279N
- Button (calibration) – micro switch
- 2x buttons (move enable, new full syringe) – micro switch

Mechanical parts:

- Threaded rod
- Coupler
- 2x linear bearings
- Metal rod
- Ball bearing

3D printed parts:

- EndIdler
- EndMotor
- Follower
- Syringe holder middle
- Syringe holder end

- Top servo (air flow control)
- Down servo (air flow control)

5.2.2 Software

Individual parts of the dispensing system (stepper motor, servo, and LEDs) are determined by the SyringeControl class, which defines their behavior. Inputs are buttons and their functions are described in the diagram below 5.6.

The servo uses PWM to control, a problem with asynchronous PWM output appeared during implementation, the servo started to be twitchy. The problem is that Raspberry Pi uses a software PWM clock and the time in between each pulse might be inconsistent. That was solved by using the Servo library from package gpiozero which switches several PWM outputs to hardware PWM clock.

Program works according to the state diagram in figure 5.6. The diagram depicts the calibration process which is important for detecting the initial position of the stepper motor. It is important to mention that when the program is in the spraying state, there is current in the stepper motor which prevents hand rotation. On the other hand, the current which goes through the stepper motor is not zero and in the long run it could damage the stepper motor or controller.

The stepper motor uses half step moves for smoother and more precise movements. The implemented stepper controller does not provide microstepping which is a standard control of stepper motors, it is already implemented in the second prototype.

Diagram 5.6 is a general state diagram but in real implementation, multiprocessing is used for syringe control, main process reads the control button which outputs whether the new syringe was inserted. The State machine is applied for the main process, shown in diagram 5.7 and the individual states and transitions are described bellow.

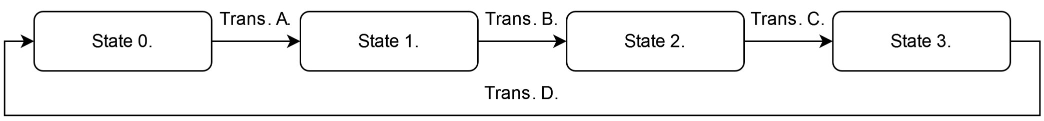

Figure 5.7. Dispensing system - main process state diagram

States:

- State 0. – Going to the initial position
- State 1. – Check the initial position
- State 2. – Spraying
- State 3. – Wait 1s

Transitions:

- Trans. A – Full syringe button is pressed
- Trans. B – Move is finished, Air control servo is in position On
- Trans. C – Move is finished
- Trans. D – No air goes out of the tube, Air control servo is in position Off

Two buttons are used for control. The first one is called *MoveEnable* which has to be pressed for every move, also in-build LED light shows when it is possible to press this button to make any movement. In other words, the LED indicate that the main process is in the Spraying state. The second button, called *NewSyringe* can be pressed when the main thread is in the 0. state, and the insert LED, on the device's cover, is

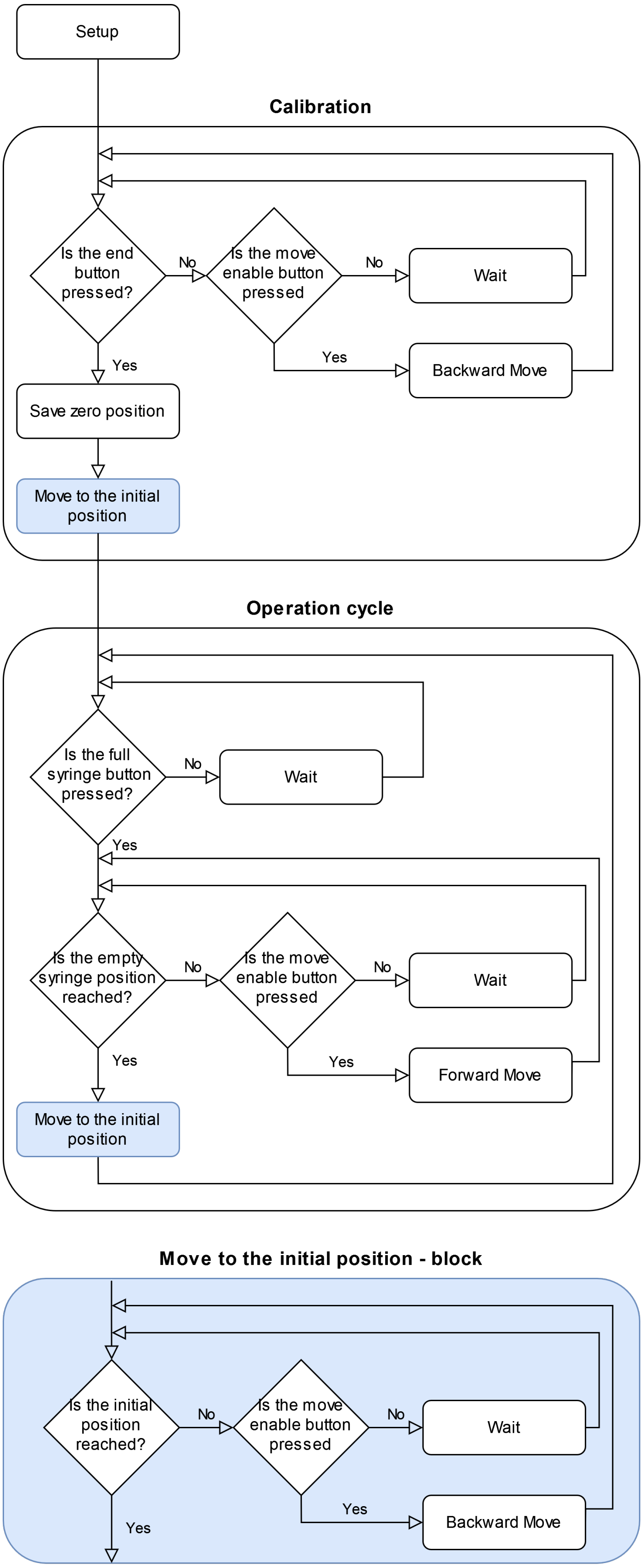

Figure 5.6. Dispensing system - software diagram

turn on. Pressing the *NewSyringe* button gives a signal to the state machine that a full syringe was inserted and the spraying can start again. This button starts new spraying circle.

5.2.3 Signaling system

A few parameters are measured and it is important to visualize them in some proper way for surgeons. For good usability is important to keep in mind that the surgeon has to, for most of the time, look at the currently sprayed wounded body part. Showing information on an external display would be distracting. Using LED on the hand-held device could cause the same issue and distract the surgeon, but this type of visualization is used in the first prototype, mainly because of easy integration.

The idea of how to show the most important data is to project the data on the treated body. The important data in this prototype are for example, showing that the surgeon is out of the distance limit. If that happens, the projected light will start pulsing softly to inform the surgeon that some of the measured parameters are not being followed.

The first prototype solely uses a white power LED which is placed in a 3D printed tube, it would be way better to use proper lenses to make the same effect but time pressure required me to come up with an improvised solution. It is used for signaling distance in Z-axis. Figure 5.8 shows the behavior of the LED for different error values from the correct one.

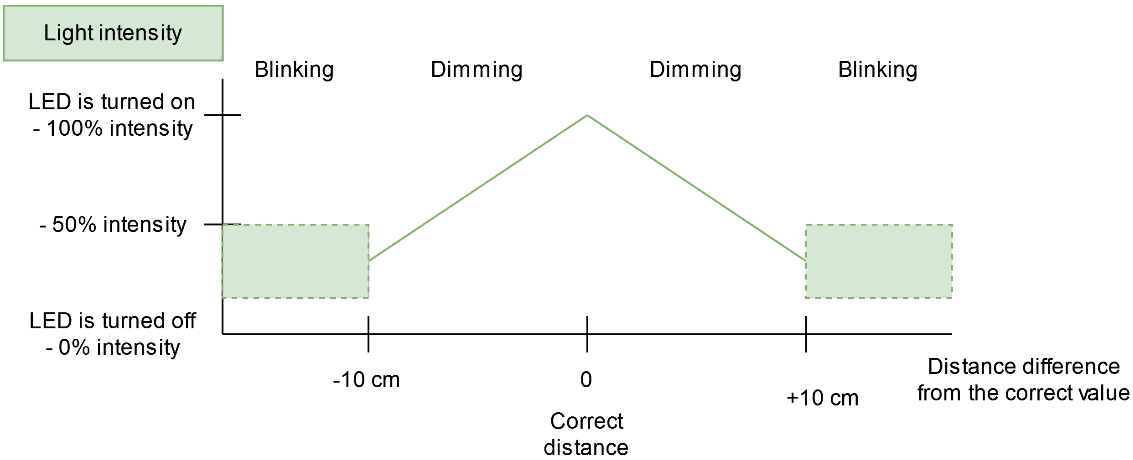

Figure 5.8. LED behavior for different distance errors

As mentioned prior, several LEDs were used, one power LED which shows the behavior for different distance errors, and five LED's which report the current state of the main thread.

The following lists show the purposes of individual LEDs.

- Yellow "ON" LED: It is turned on when the program is running, dimmed during motor calibration
- Blue "Insert" LED: Turned on when syringe can be changed for the full one
- Green "–" LED: Signalize that the sprayer is too far from the target distance
- Red "+" LED: Signalize that the sprayer is too close from the target distance
- Blue Button LED: Shows when the prototype is in move mode

5.3 The second prototype

The second prototype 5.9 inherits many functions from the first one. It was developed with the purpose to use the device in practice at least in laboratory conditions and gather data from surgeons on what should be improved in the next prototype. The prototype is reliable and has all the necessary functions for the medication. The prototype has just a few additional functions in comparison with the first one, however, these functions are essential for our application.

The prototype helps with applying medication and choosing the right speed for distributing the medication. It uses a custom-designed laser system that indicates the distance from the body wound and spraying nozzle profile.

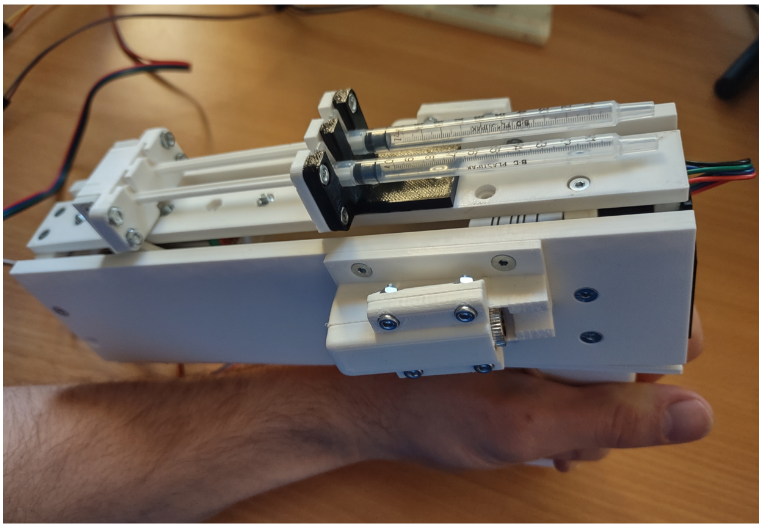

Figure 5.9. The second prototype

5.3.1 Linear stage

The linear stage is used for precise dosing of the medication. The linear stage uses a stepper motor and threaded rod for moving, similar to the first prototype. The main improvement is in the supporting system. While the first prototype uses two aluminum rods with bearings, this system was replaced by a rail with a cart 5.10. The system enabled making the whole structure smaller and more compact, with big potential to make it even smaller in the future prototypes. Figure 5.11 shows the 3D model prototypes comparison.

The next big difference is the stepper motor controller. Firstly, I tried to use the stepper controller Trinamic tmc2130 which has a feature called StallGuard2 that measures the mechanical load of the motor and can work as an end button. The end button sets the initial position of the stepper motor and the feature makes the device even smaller. Unfortunately, I was not able to make this feature functional. Instead, the A4988 motor controller is used, but it is possible to change it very easily because both controllers have the same pinout. The calibration has not been solved and the user has to set the first position manually.

5.3.2 Laser system

A custom-designed laser system is used for distance detection and visualization. The first prototype uses a ToF sensor and power LED which needs additional hardware for

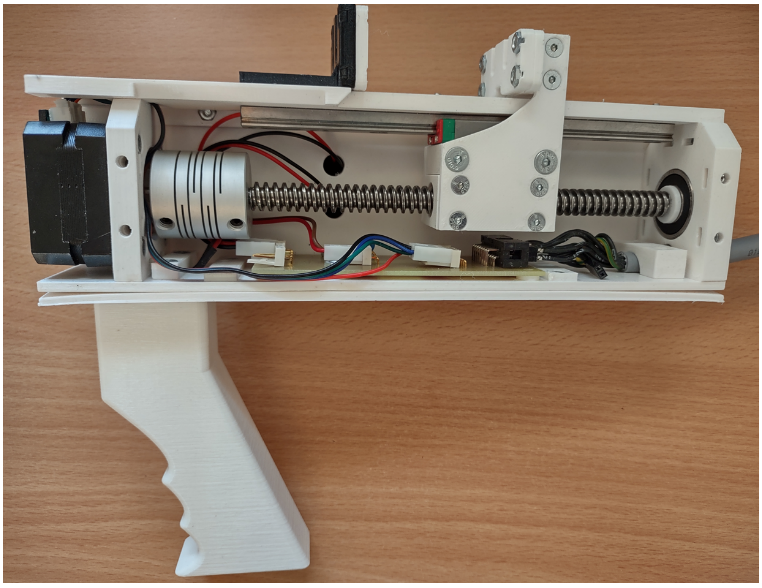

Figure 5.10. The second prototype linear stage

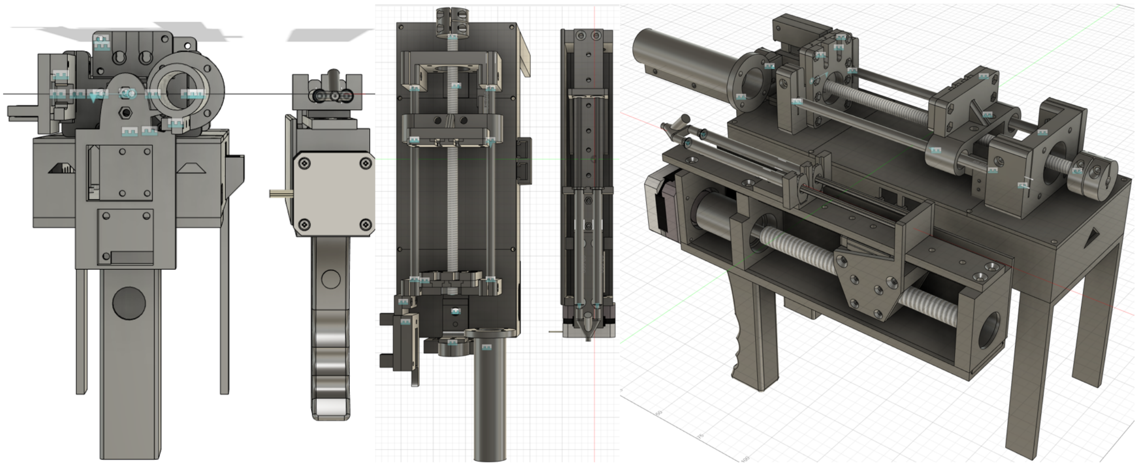

Figure 5.11. 3D model prototypes comparison

controlling and visualization. The second prototype uses a solution which is inspired by SpinCare device.

In the first stage of development, dot lasers were implemented. This solution is shown in the figure 5.13. It helps with the navigation in very elegant way without any additional hardware and software. However, it lack information about the angle in between the sprayer and the body. It does not show the sprayer profile of the nozzle. These issues solve the second iteration of the laser system which uses laser lines 5.14.

This solution makes the complexity of the device significantly lower. And it solves the problem with visualization. When the laser lines are well designed, it shows the spraying profile of the mounted nozzle. In simpler words, it shows where exactly on the wound the device is spraying and the distance between the sprayer and the body wound is visible, the principle of the visualization is shown in figure 5.12 and it is based on the angle of laser lines in two axes.

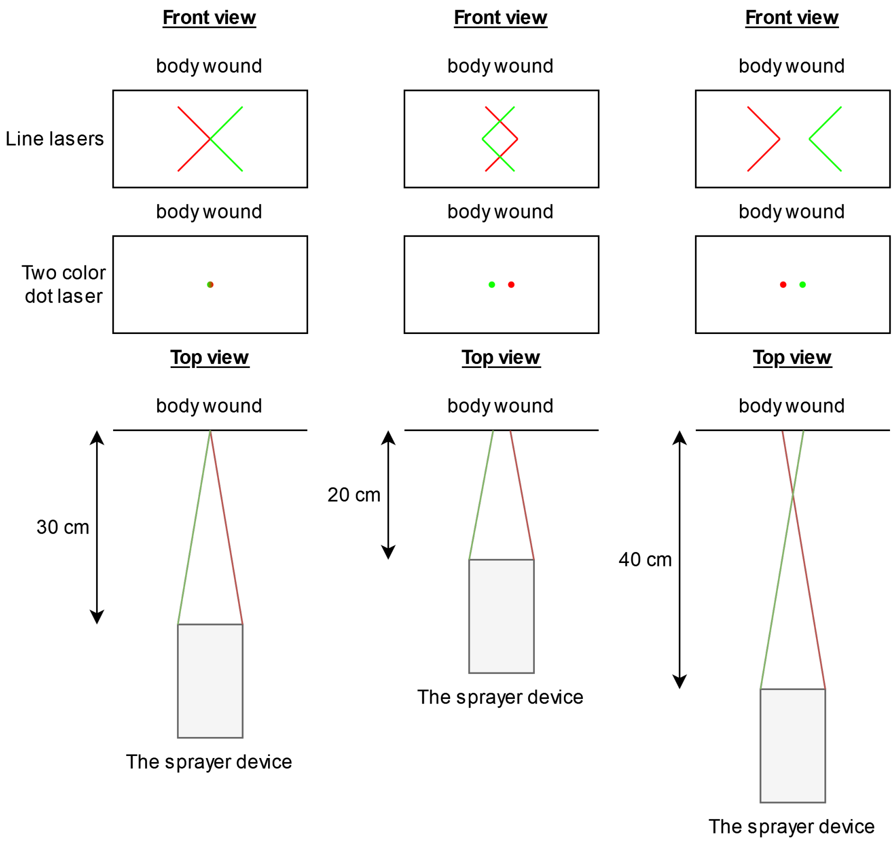

Figure 5.12. Schematic principle of the laser system

5.3.3 Mechanical improvements - Syringe holder

Standard syringe types vary a lot. Just 1 ml syringe is used during the application process right now. It is mainly because 1 ml syringes are long and surgeon does not have a problem with maintaining an even amount of pressure at the end of syringe, during applying. Meaning it is easier to use it for manual spraying, especially, when we compare them with 2 ml which is shorter and thicker.

The second prototype contains a linear stage with a very precise positioning system. With the help of that, we can use syringes that have bigger volumes. For large wounds, it would not be necessary to change the syringes every few seconds.

That is why syringe holders are individual parts that are attached to the upper holder part and can be easily changed for holders of different syringe types. In figure 5.15, you can see the four parts which hold the 1 ml syringe.

5.3.4 Mechanical improvements - Detachable handle

Among the device's practical properties, which were discussed with clinicians, is the opportunity to sanitate the device or find a solution on how to keep it clean. The developed prototype contains electronic and mechanical parts, so it is not possible to simply dip it into a sanitation liquid. Firstly, it is important to find out how different medical devices deal with this issue.

One solution can be that the surgeon will wear gloves during the spraying procedure.

A more complicated solution could be to use the mechanical handle. It is possible to detach it from the core part and clean it without the core part with electronic and mechanical parts.

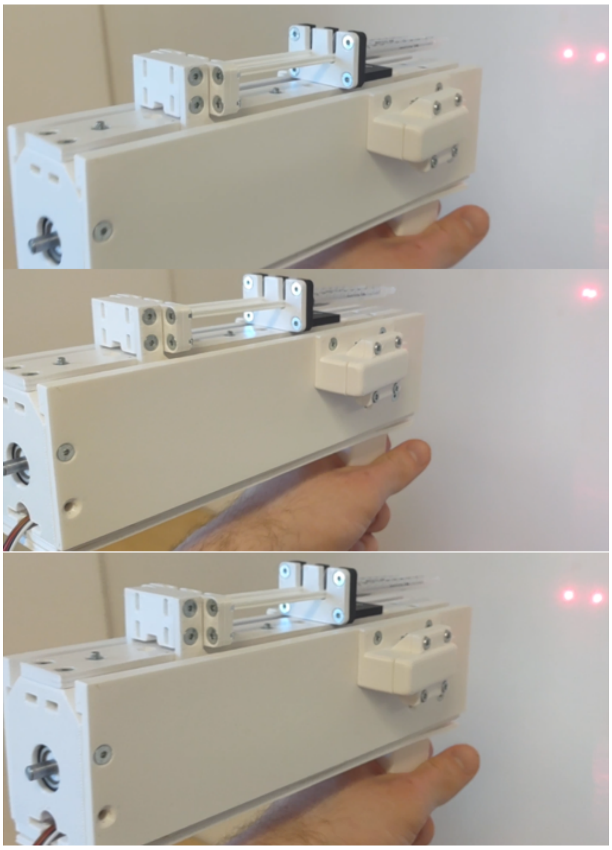

Figure 5.13. The projection laser system - dots

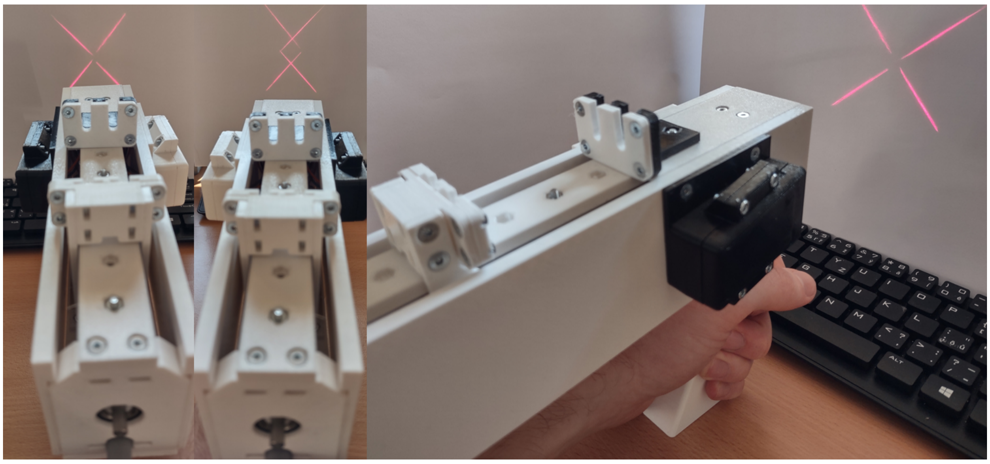

Figure 5.14. The projection laser system - lines

The problem with the disinfection of medical devices is quite a broad topic and in different countries, different rules/laws apply. But still, it was decided to try to implement some mechanism that proves that sanitation is possible. The final solution is similar to the one described above. One part of the device which is used by the surgeons can be separated and considered as a clean part and the second part of the device which contains the electronics and linear stage is considered as a dirty part and the surgeon should not touch it 5.16.

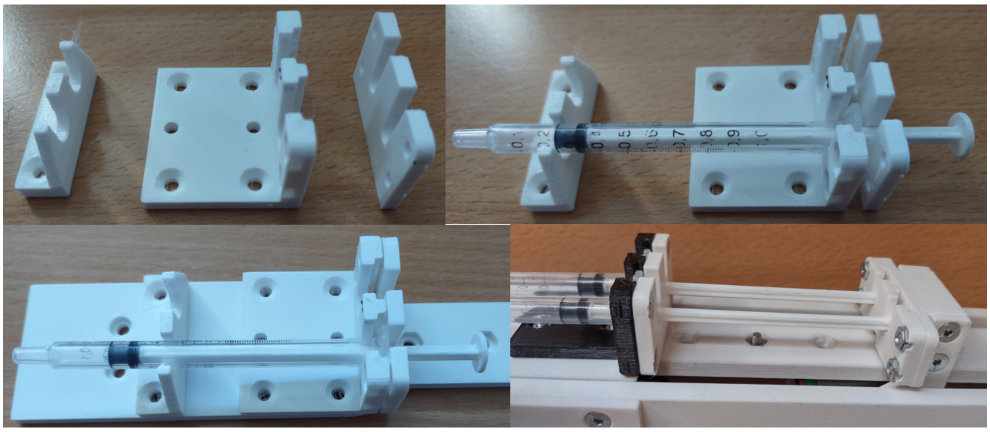

Figure 5.15. Parts of the syringe holder

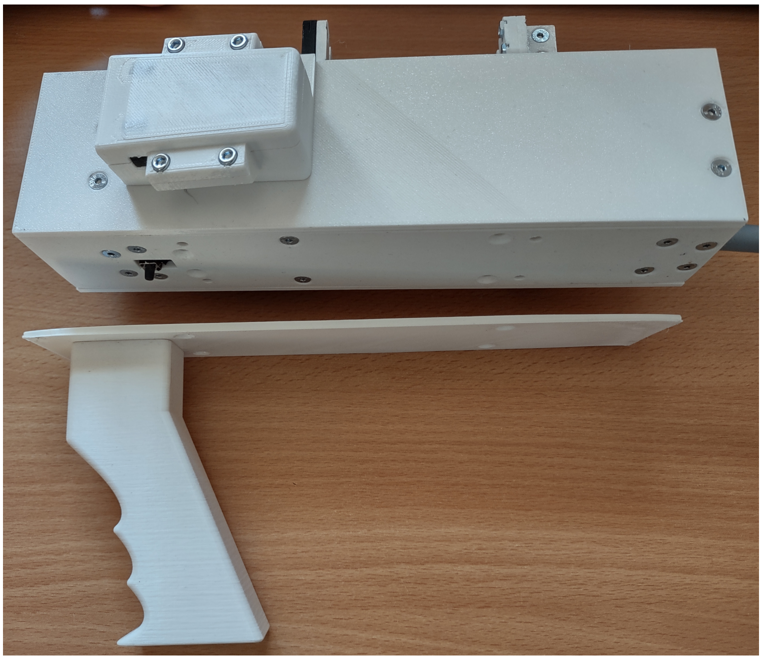

Figure 5.16. The Detachable handle of the second prototype

It is worth mentioning that the detachable handle contains a button that controls the movement of the linear stage. The trick is that the button is placed in the core part and a lever system is used for extending the button.

5.3.5 Electronics

The second prototype contains two components that require power. The system dependent solely on electrical power is the laser system. The second component, which is more complicated than the laser system, is the whole control of the linear stage. The linear stage needs several components, a stepper motor, a stepper motor controller, a micro-controller that sends pulses to the stepper motor controller, and a button that controls the movement of the stage. Both of these components require power supply. Everything is visible in figure 5.17.

The first prototype has all the electronics inside of the sprayer, the core body. It makes it bulky and hard to manipulate, which is against one of the project's priorities.

To make the second prototype smaller and easier to manipulate, it was decided to separate the electronics and place the control hardware into an external box.

Two electronic parts are the result of the separation. The main part is in the external box and only the essential components are still in the hand-held device, these two parts are connected via cable. One of the motivations for the separation was to use the core of the device for the next, third prototype which is going to have a depth camera. Data from the depth camera is not possible to evaluate inside of the hopefully small in-hand sprayer device. It would end up being too large.

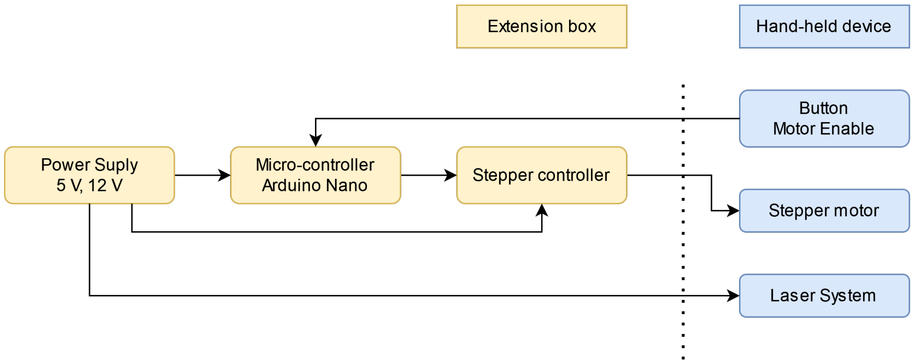

Figure 5.17. Schematic design of electronics in the second prototype

As was mentioned above and in figure 5.17, the electronics are divided into two parts: the external board and the conjunction board.

The external board contains control electronics such as micro-controller, stepper motor driver, and supported hardware, a schematic diagram shows the components in detail 5.18. The brain of the sprayer is a micro-controller Arduino Nano Every. It controls the stepper motor and is prepared for LED strip control, which can be used as an additional visualization tool. A PCB was made and the result together with components is shown in figure 5.19 it is also placed in a custom-designed and 3D printed box.

The conjunction board works as a hub that connects the sprayer and the external board, there is a wire connecting these two parts. The implemented conjunction board is visible in figure 5.10 above.

Figure 5.19. External board realization with components

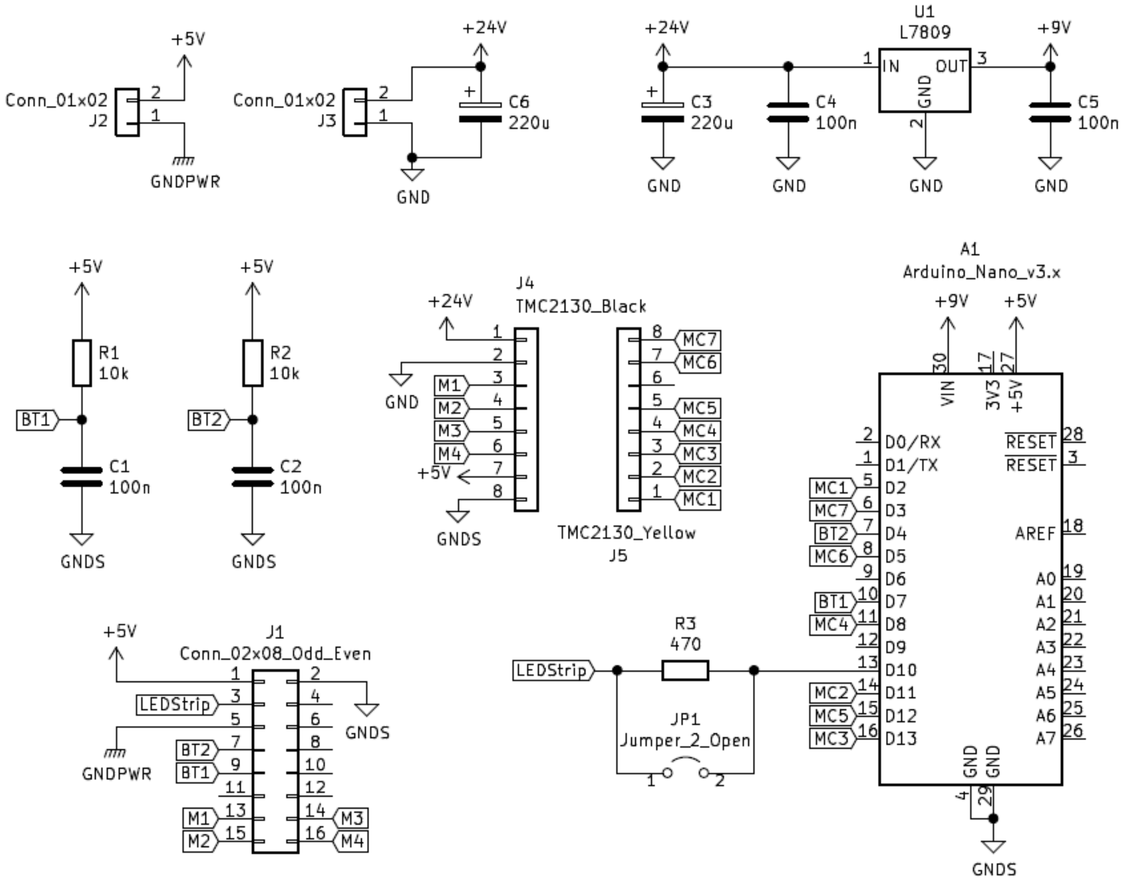

Figure 5.18. External board schematic diagram

5.3.6 Software

Only the micro-controller has the possibility to be programmed. The software for the second prototype is not as extensive as the software for the first prototype. In this case, just linear stage control is implemented. Automatically setting the zero position of the stepper motor is not accomplished yet, it is mainly because of the missing end button and plans to use the stepper controller with the feature StallGuard2.

There are two options to determine the zero position of the stepper motor. The first one can be called a manual set. Before the program starts, the zero position is set by rotating the threaded rod until the position of the syringe end holder is in place. Then, it is possible to insert a full syringe. Another option is to start the program, press the button and let the holder for the syringe end go forward. When it hits the middle syringe holder, the stepper motor starts to skip steps. When we wait until the end of the forward movement, the backward move begins and the end syringe holder will be in the right place for inserting a full syringe.

The program for linear stage movement contains two main numbers which determine the number of steps needed to reach two different positions. The first position is for inserting a full syringe and the second determines when the syringe is empty. The first position is always zero and according to measurements, the second position is set. In other words, the second position informs how many steps are necessary to empty the syringes.

The program is ready for LED strip implementation, which could work as an additional signaling system. This system would require a few prototype tests because proper optics would have to be calculated. But even with this possibility, no data in this prototype could be visualized. This feature can be implemented in the next prototype.

Chapter 6
Prototypes evaluation

In this chapter, prototypes which were build are evaluated and results of tests are presented.

6.1 The first prototype

This prototype was built with a goal to prove the concept of hand held device. It uses time of flight sensor which was evaluated in during sensor testing 4.1.5. The signaling system shows measured data based on the description in section 5.2.3. There is space for improvements mainly in the light projection. It is good to mention that the first prototype require more testing which could show the main drawbacks of the device.

6.1.1 Surgeon's feedback

Even with little testing of this prototype, several improvements needed were found. These potential improvements needed to be implemented for better results that fulfill requirements for use during burn surgeries.

The first prototype was presented at Jorvi's Helsinki University Hospital (HUS) and a discussion with surgeons and nurses provided several ideas on how to improve the device.

The first outcome is to prioritize developing a signaling system and show the measured distance clearly. Here it was first mentioned that the distance does not have to be measured but showing it properly by using lasers can be sufficient.

The main ideas were:

- Laser circle with cross in the middle
- The circle match with nozzle spray profile

In the end, this system was implemented in the second prototype.

The size and weight of the device were the next concerns of the surgeons. Future development should be focused on making the device lighter and placing the computational part in a different case and not directly inside the hand-held device.

Sterilization was a big topic of the visit but surgeons and nurses said that it should not pose a problem. But it is important to keep the sterilization in mind.

Improvements that would be great to make:

- Laser distance measurement system
- Separate the hand-held device and computational HW and make two different devices connected by wire.
- Use better stepper controller
- Make the handle ergonomic
- Hide the mechanical parts of the linear stage

6.2 The second prototype

This prototype contains several systems which can be tested. The laser system and linear stage have been tested.

6.2.1 Laser system test

The goal of the test is to compare laser signaling system which the prototype uses with simulated laser system.

The simulation of the laser signaling system is done in open source software Open-SCAD which allows parametric 3D objects design. The simulation uses four laser lines and projection plane, figure 6.1 shows the whole setup.

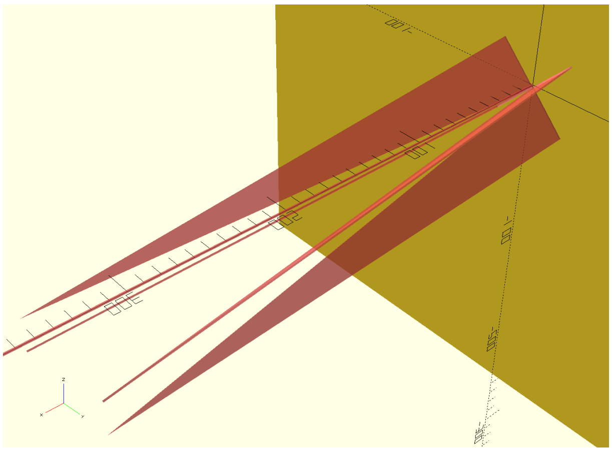

Figure 6.1. Test of the laser system - simulation

Parameters of the laser lines were determined based on trigonometric equations and tuned to show the laser lines based on specification given by figure 5.12. Figure 6.2 shows the parameters in the 3D model:

Following parameters was important to set:

- The angle of the laser ray $\alpha = 6°$
- The angle in X-Y plane $\beta = 4°$
- The angle in Y-Z plane $\gamma_1 = 5°, \gamma_2 = 4.4°$

Evaluation of the prototype was done by using setup showed in figure 6.3. The prototype projects laser lines on the paper with a scale. The tape measure is used to set the correct distance in between the paper and device.

Figure 6.4 shows the comparison of the projected laser lines in simulation and by the prototype for different distances d in between sprayer and projected plane. The projection of the prototype is almost similar with the simulation. Main imperfections are caused by the plastic components which were 3D printed and their precision is not as high as the laser system requires.

6.2.2 Linear stage test

The goal of this test is to prove that the movement speed of the linear stage corresponds with the values in code.

The control software contains a few parameters listed bellow which are necessary to know for calculating the movement speed of the linear stage:

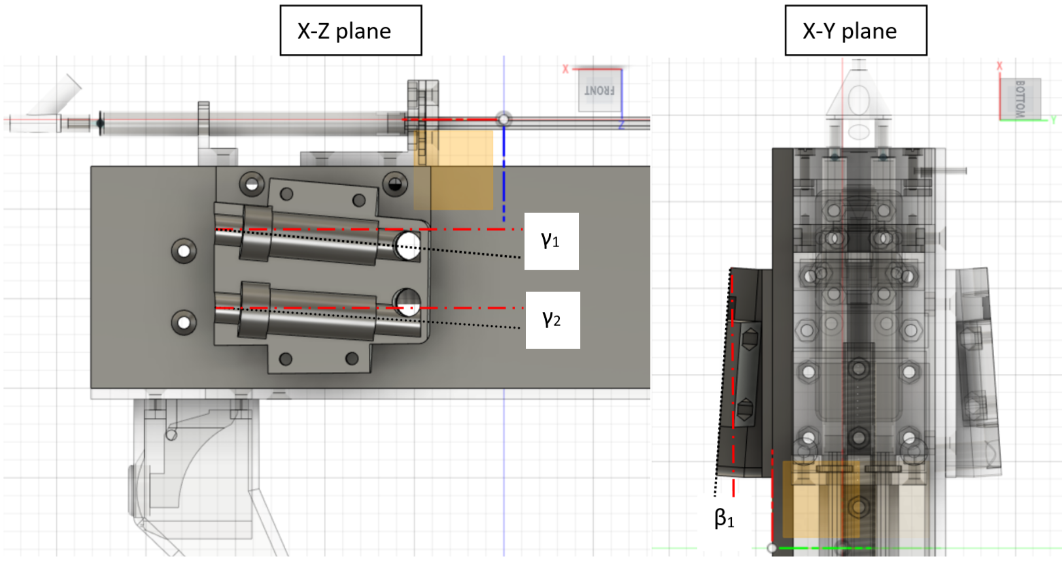

Figure 6.2. Test of the laser system - important parameters

Figure 6.3. Test of the laser system - real setup

- Steps per revolution $Steps = 200$
- Revolutions for 1 ml syringe $Revs = 40$
- Delay between steps (forward and backward movement) $t_f = 2ms, t_b = 1ms$

Time for emptying syringe tc_e and time for returning stage to the initial position tc_b are possible to calculate by using these equations:

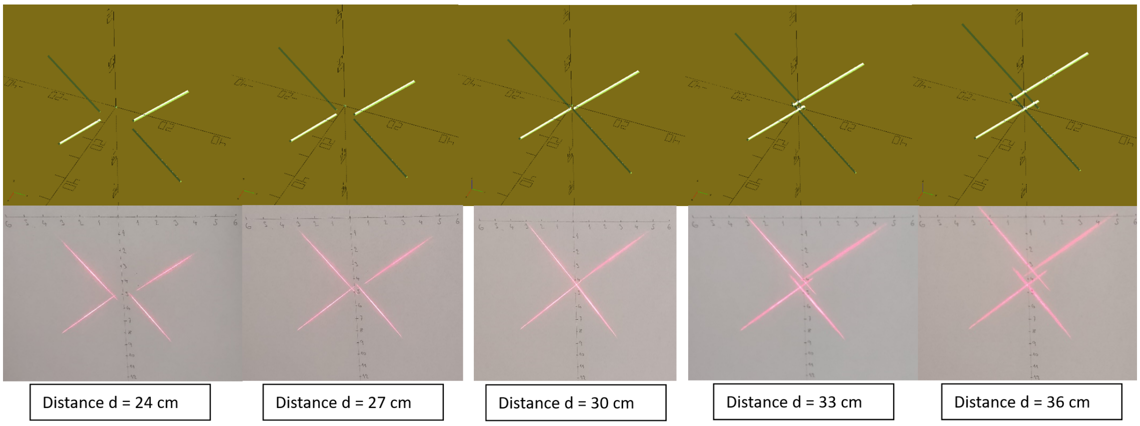

Figure 6.4. Test of the laser system - results

$$tc_f = Steps \cdot Revs \cdot t_f = 200 \cdot 40 \cdot 2 = 16\ s$$

$$tc_b = Steps \cdot Revs \cdot t_b = 200 \cdot 40 \cdot 1 = 8s$$

Test on the second prototype have been done by capturing movement and measuring time. A few frames of the video is shown by figure 6.5. It shows that the forward time is $tt_e = 16$ s and the backward time is $tt_b = 10$ s. This values roughly corresponds with the calculated values. The error can be caused by different operations of the microcontroller.

6.2.3 Surgeon's feedback

The second prototype was designed and made in the Czech Republic. Thanks to the visit to Jorvi's hospital and the surgeons' connections, I got the opportunity to discuss imperfections with surgeons from the burn center in Prague. We agreed that making the device even smaller should be one of the main centers of attention. Also, the imbalance of the handle should be solved, because right now most of the mass is on the end.

During the visit, I got my hands on the SpinCare device and one feature could be adopted, which is the two control button. The first one turns on the laser pointers and the second one moves the linear stage.

The last important outcome discussed was whether surgeons prioritize and would rather visualize the movement speed or the already applied layer of medication. The answer was not black and white because both pieces of information are important. But according to the surgeon from the Prague burn center, they would rather visualize the layer of applied medication. However before jumping to conclusions, it is better to try both and let the surgeons make the decision.

Possible improvements for the next prototypes:

- Make the device smaller and good balanced
- Visualize movement speed and the layer of already applied medication
- Use two control buttons
- Use a depth camera as a 3D scanner
- Add visualization by using LED strips

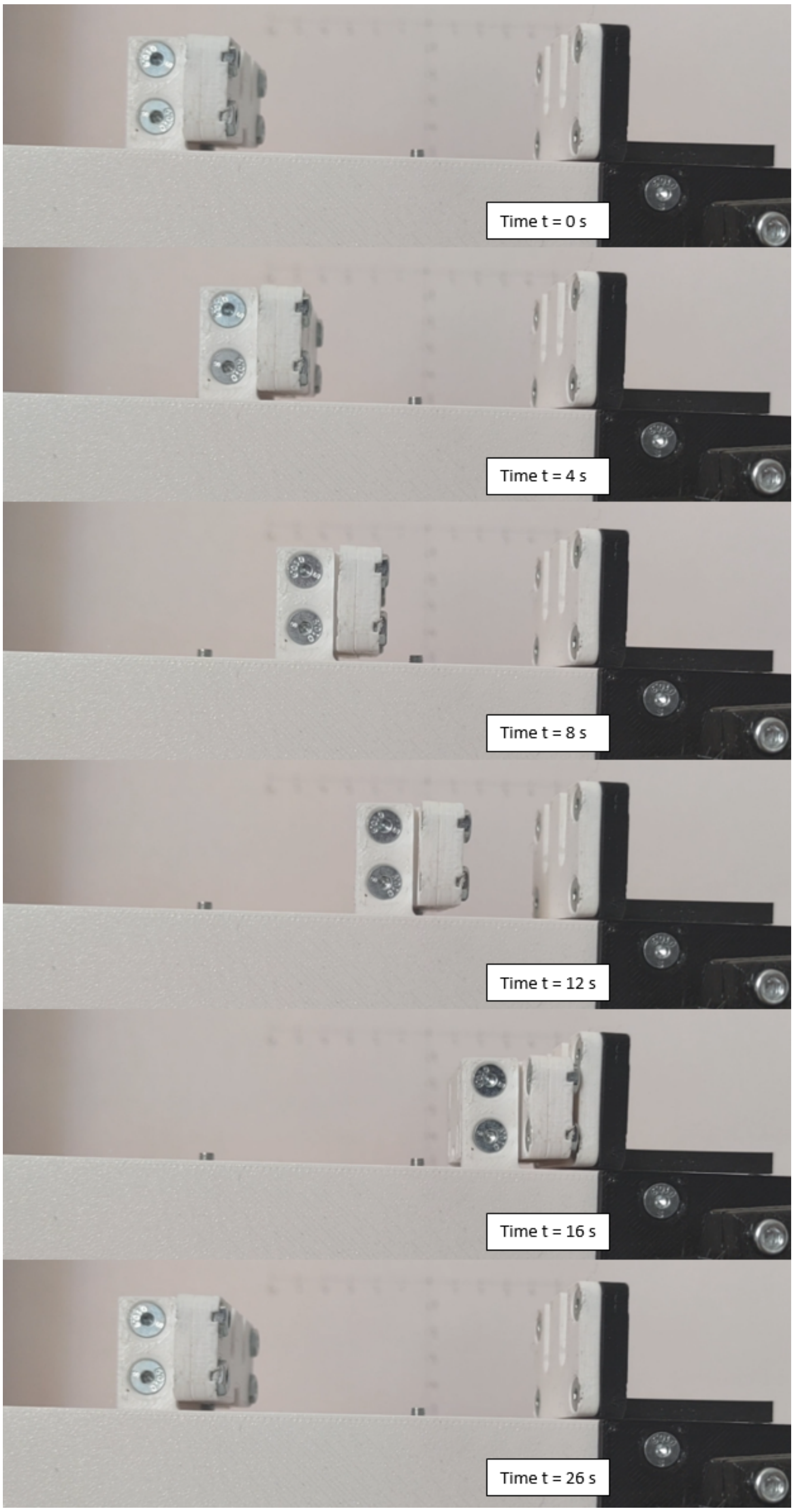

Figure 6.5. Test of the linear stage

Chapter 7
Discussion

In the introduction chapter we tried to find the best sensors or measurement techniques for measuring important parameters of the applying process. A few tests of the individual problems were done in the validation section. These tests reveal that it is hard to find an ideal solution for all tasks together, but it is possible to evaluate the results of each problem individually.

The best sensor for distance measurement is the time of flight sensor, because it provides reasonably accurate data even in harder conditions (the measurement of curved surface 4.1.6) in comparison with ultrasound measurement. It almost does not rely on lighting conditions, in comparison with methods that use a camera. Also, there is no change in results caused by spraying 4.3. But a few tests should be done to test the quality of individual time of flight sensors. Additionally, different reflection materials should be tested.

Sensors in general require the use of additional hardware and signaling systems. That is the reason why the second prototype uses a laser system to detect distance 5.3.2. There is a big issue with the red laser lines which are used. During surgery the red lines could be invisible because of the strong lighting system in operation rooms, green lasers should be used instead. This non sensor strategy makes the size of the device much larger. One possible solution would be to integrate the laser system and place it inside the sprayer. However, there would be a certain problem with resolution. This problem has to be solved for the next prototypes.

The speed detection, which is essential for application, was not tested properly. But there are a few outcomes to take into consideration for future development of the device. First of all, using an inertial measurement unit alone is not an ideal solution. That is so because it is possible to estimate the speed out of it, but the measurement is not reliable because of the drift caused by the earth's gravity 4.10. The second outcome is that camera speed detection is reliable and it would be helpful to focus on it in future development 4.3. The most beneficial improvement would be to try camera feature detection with the wound surface and discover if there are some detectable features to make this method reliable.

Orientation detection was not properly tested. The importance of it is not essential for the application of medication and this attribute is not hard to maintain by the surgeon. Also, I have not found a reliable solution yet, except for the camera solution.

Two prototypes were been built. The first one proves that such a device is possible to create 5.3. Distance measurement is maintained by the time of flight sensor and visualized by two options, either by using the color LED lights on the side of the prototype or by using power LED white light, which is projected on the patient's wound 5.8. It also contains a camera that streams the front view. A basic linear stage is used for pushing medication out of the syringes.

The second prototype does not contain any sensor, the distance is visualized by a laser system which also shows the nozzle spraying profile 5.14. Tests of the laser signaling system shows the precision of the system 6.2.1. If different material would be used the precision could be higher. The linear stage is significantly smaller in comparison with the first prototype and the movement precision is higher. But even the linear stage and all mechanical parts require improvement, an ergonomic handle would be great to make, and the overall design should be more compact. Figure 5.10 shows that there is still lots of wasted space, for example, the coupler and width of PCB.

The surgeon's feedback is one of the key outcome of the thesis, as based on it is possible to create a device that best fits their needs 6.1.1, 6.2.3. Both discussions shared concerns about the weight and size of the device, this topic should be solved in the following development stages.

However, the goal of the project and thesis itself was to design and build a device that works and shows the surgeons that such a device is possible to make and use during surgery. It is important to mention that it would be ideal if all problems were researched in more detail.

Chapter 8
Conclusion

The task is more complex than it can look on the first sign. First of all, the project's goal was not specific, there were some boundaries, but it was unknown what kind of solution was the best. Two concepts were tested. The first prototype is almost a standalone device, and the second prototype is lighter but requires an additional external box and cable, which can generate many complications.

The prototypes are based on knowledge gained from measurements showing several aspects that needed to be more straightforward. For example, position estimation based on data from an inertial measurement unit is difficult to process. Article [25] claims that it is possible, but all these topics require experts in the fields.

It is important to mention that the project was started from scratch. The only instructions were to build a cell therapy device that measures distance, movement speed, and orientation. The first concept tests with structured light started. Afterward, we evaluated the results and decided what the next steps should be, and lots of iterations of this approach were made until the prototype was ready.

All steps required knowledge from several fields: general medical view, just to know that it is important to solve sanitation. Also, mechanical engineering was important for designing the linear stage and the whole structure of the prototypes. And the last field was electrical engineering, which was necessary for all sensory tests, PCB design, and writing code. Just one person with the help of many consultants completed all of the described work, which is why not everything is perfect.

The project has the potential to grow because there is no proper device for cell therapies on the market. With the newly gained knowledge, it would be possible to develop it further and build the third prototype, which will be possible to use in practice and hopefully help surgeons save lives.

References

[1] Jaclyn M McBride, Kathleen S Romanowski, Soman Sen, Tina L Palmieri, and David G Greenhalgh. Contact Hand Burns in Children. *Journal of Burn Care & Research*. 2020-09-23, 41 (5), 1000-1003. DOI 10.1093/jbcr/iraa102.

[2] Donghui Bian, Yan Wu, Guodong Song, Ramyar Azizi, and Amir Zamani. The application of mesenchymal stromal cells (MSCs) and their derivative exosome in skin wound healing. *Stem Cell Research & Therapy*. 2022, 13 (1), DOI 10.1186/s13287-021-02697-9.

[3] *What is the skin?* 2023.
https://www.clinimed.co.uk/wound-care/wound-essentials/structure-and-function-of-the-skin.

[4] Marc G. Jeschke, Margriet E. van Baar, Mashkoor A. Choudhry, Kevin K. Chung, Nicole S. Gibran, and Sarvesh Logsetty. Burn injury. *Nature Reviews Disease Primers*. 2020, 6 (1), DOI 10.1038/s41572-020-0145-5.

[5] *Burns*. 2015.
https://www.bapras.org.uk/public/patient-information/surgery-guides/burns.

[6] Bishara S. Atiyeh, S. William Gunn, and Shady N. Hayek. State of the Art in Burn Treatment. *World Journal of Surgery*. 2005, 29 (2), 131-148. DOI 10.1007/s00268-004-1082-2.

[7] James Hill Holmes IV, Joseph A Molnar, Jeffrey E Carter, James Hwang, Bruce A Cairns, Booker T King, David J Smith, C Wayne Cruse, Kevin N Foster, Michael D Peck, Rajiv Sood, Michael J Feldman, Marion H Jordan, David W Mozingo, David G Greenhalgh, Tina L Palmieri, John A Griswold, Sharmila Dissanaike, and William L Hickerson. A Comparative Study of the ReCell® Device and Autologous Split-Thickness Meshed Skin Graft in the Treatment of Acute Burn Injuries. *Journal of Burn Care & Research*. 2018-09-17, 39 (5), 694-702. DOI 10.1093/jbcr/iry029.

[8] G. Gravante, M.C. Di Fede, A. Araco, M. Grimaldi, B. De Angelis, A. Arpino, V. Cervelli, and A. Montone. A randomized trial comparing ReCell® system of epidermal cells delivery versus classic skin grafts for the treatment of deep partial thickness burns. *Burns*. 2007, 33 (8), 966-972. DOI 10.1016/j.burns.2007.04.011.

[9] A. Schulz, P.C. Fuchs, W. Heitzmann, C.H. Kanho, and J.L. Schiefer. Our Initial Experience In The Customized Treatment Of Donor Site And Burn Wounds With A New Nanofibrous Temporary Epidermal Layer. *Ann Burns Fire Disasters*. 2021, 2021 (34(1)), 58-66.

[10] *Spincare*.
https://www.regenmedical.co.uk/products/nanomedic/.

[11] *Inside the Lab Building a Stem Cell Gun to Heal Skin*. 2022.
https://www.labiotech.eu/interview/stem-cell-gun-renovacare/.

[12] *EASYSPRAY Quick Reference Guide (for open wound surgery)*. 2015.
https://www.hpra.ie/docs/default-source/3rd-party-documents/educational-materials/tisseel_hcp_easyspray-qrg_v1-07-15.pdf?sfvrsn=4.

[13] Berthold K.P. Horn, and Brian G. Schunck. Determining optical flow. *Artificial Intelligence*. 1981, 17 (1-3), 185-203. DOI 10.1016/0004-3702(81)90024-2.

[14] Johanes L. Schonberger, and Jan-Michael Frahm. Structure-From-Motion Revisited. *Proceedings of the IEEE Conference on Computer Vision and Pattern Recognition (CVPR)*. 2016, 4104-4113.

[15] Ilmir Z. Ibragimov, and Ilya M. Afanasyev. Comparison of ROS-based Visual SLAM methods in homogeneous indoor environment. *14th Workshop on Positioning, Navigation and Communications (WPNC)*. 2017,

[16] Alessandro Filippeschi, Norbert Schmitz, Markus Miezal, Gabriele Bleser, Emanuele Ruffaldi, and Didier Stricker. Survey of Motion Tracking Methods Based on Inertial Sensors. *Sensors*. 2017, 17 (6), DOI 10.3390/s17061257.

[17] César Debeunne, and Damien Vivet. A Review of Visual-LiDAR Fusion based SLAM. *Sensors*. 2020, 20 (7), DOI 10.3390/s20072068.

[18] Shengze Cai, Shichao Zhou, Chao Xu, and Qi Gao. Dense motion estimation of particle images via a convolutional neural network. *Experiments in Fluids*. 2019, 60 (4), DOI 10.1007/s00348-019-2717-2.

[19] *Cardiac catheterization*. 2021.
https://www.mayoclinic.org/tests-procedures/cardiac-catheterization/about/pac-20384695.

[20] Thuong N. Hoang, Hasan S. Ferdous, Frank Vetere, and Martin Reinoso. *Body as a Canvas.* In: *Proceedings of the 2018 Designing Interactive Systems Conference*. New York, NY, USA: ACM, 2018-06-08. 253-263. ISBN 9781450351980.
https://dl.acm.org/doi/10.1145/3196709.3196724.

[21] Bas Wijnen, Emily J. Hunt, Gerald C. Anzalone, Joshua M. Pearce, and Giorgio F. Gilestro. Open-Source Syringe Pump Library. *PLoS ONE*. 2014-9-17, 9 (9), DOI 10.1371/journal.pone.0107216.

[22] *Terufusion™ Syringe Pump (Smart)*.
https://www.terumo-europe.com/en-emea/products/terufusion%E2%84%A2-syringe-pump-(smart).

[23] *Time of flight*. 2001-2023.
https://en.wikipedia.org/wiki/Time_of_flight.

[24] Ti-Ho Wang, Ming-Chih Lu, Wei-Yen Wang, and Cheng-Yen Tsai. Distance measurement using single non-metric CCD camera. *Proceedings of the 7th WSEAS International Conference on Signal Processing, Computational Geometry & Artificial Vision*. 2007, ISCGAV'07 1-6. DOI 10.5555/1364592.1364593.

[25] Sebastian O. H. Madgwick. *AHRS algorithms and calibration solutions to facilitate new applications using low-cost MEMS*. 2014.

[26] xioTechonologies. *Fusion Algorithm*. 2023.
https://github.com/xioTechnologies/Fusion.

[27] Jie Yang, Alexander Varshavsky, Hongbo Liu, Yingying Chen, and Marco Gruteser. *Accuracy characterization of cell tower localization.* In: *Proceedings of the 12th ACM international conference on Ubiquitous computing*. New York, NY, USA: ACM, 2010-09-26. 223-226. ISBN 9781605588438.
https://dl.acm.org/doi/10.1145/1864349.1864384.

[28] Yapeng Wang, Xu Yang, Yutian Zhao, Yue Liu, and L. Cuthbert. *Bluetooth positioning using RSSI and triangulation methods.* In: *2013 IEEE 10th Consumer Communications and Networking Conference (CCNC).* IEEE, 2013. 837-842. ISBN 978-1-4673-3133-3.
`http://ieeexplore.ieee.org/document/6488558/`.

[29] Diederik Hermsen. *Virtual Reality (VR) tracking explained.*
`https://unboundxr.eu/hoe-vr-tracking-werkt`.

[30] Jianping Wu, Zhaobin Liu, Jinxiang Li, Caidong Gu, Maoxin Si, and Fangyong Tan. *An algorithm for automatic vehicle speed detection using video camera.* In: *2009 4th International Conference on Computer Science & Education.* IEEE, 2009. 193-196. ISBN 978-1-4244-3520-3.
`http://ieeexplore.ieee.org/document/5228496/`.

[31] Osman Ibrahim, Hazem ElGendy, and Ahmed M. ElShafee. Speed Detection Camera System using Image ProcessingTechniques on Video Streams. *International journal of computer and electrical engineering.* 2011, 3 (6),

[32] C. Chen, and A. Kak. *Modeling and calibration of a structured light scanner for 3-D robot vision.* In: *Proceedings. 1987 IEEE International Conference on Robotics and Automation.* Institute of Electrical and Electronics Engineers, 1987. 807-815.
`http://ieeexplore.ieee.org/document/1087958/`.

[33] Lei Yang, Yanhong Liu, and Jinzhu Peng. Advances techniques of the structured light sensing in intelligent welding robots. *The International Journal of Advanced Manufacturing Technology.* 2020, 110 (3-4), 1027-1046. DOI 10.1007/s00170-020-05524-2.

[34] Chadi Albitar, Pierre Graebling, and Christophe Doignon. *Robust Structured Light Coding for 3D Reconstruction.* In: *2007 IEEE 11th International Conference on Computer Vision.* IEEE, 2007. 1-6. ISBN 978-1-4244-1630-1.
`http://ieeexplore.ieee.org/document/4408982/`.

[35] Stefan Muckenhuber, Hannes Holzer, and Zrinka Bockaj. Automotive Lidar Modelling Approach Based on Material Properties and Lidar Capabilities. *Sensors.* 2020, 20 (11), DOI 10.3390/s20113309.

[36] *Camera Calibration.* 2023.
`https://docs.opencv.org/4.x/dc/dbb/tutorial_py_calibration.html`.

[37] xioTechonologies. *Oscillatory Motion Tracking With x IMU.* 2017.
`https://github.com/xioTechnologies/Oscillatory-Motion-Tracking-With-x-IMU/blob/master/Script.m`.

Appendix A
The first prototype - Schematic diagram

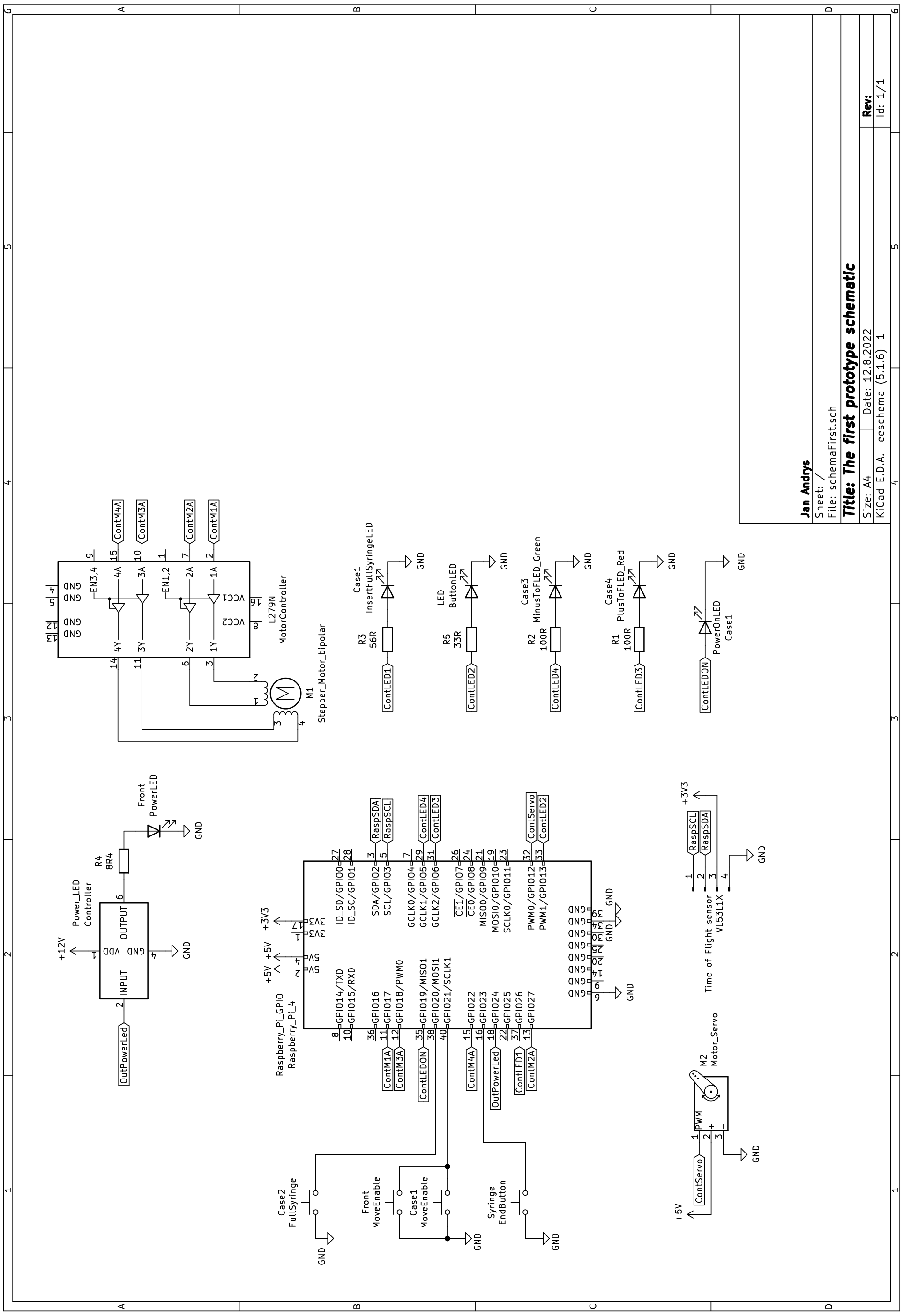

Appendix B

The second prototype - Connector Board

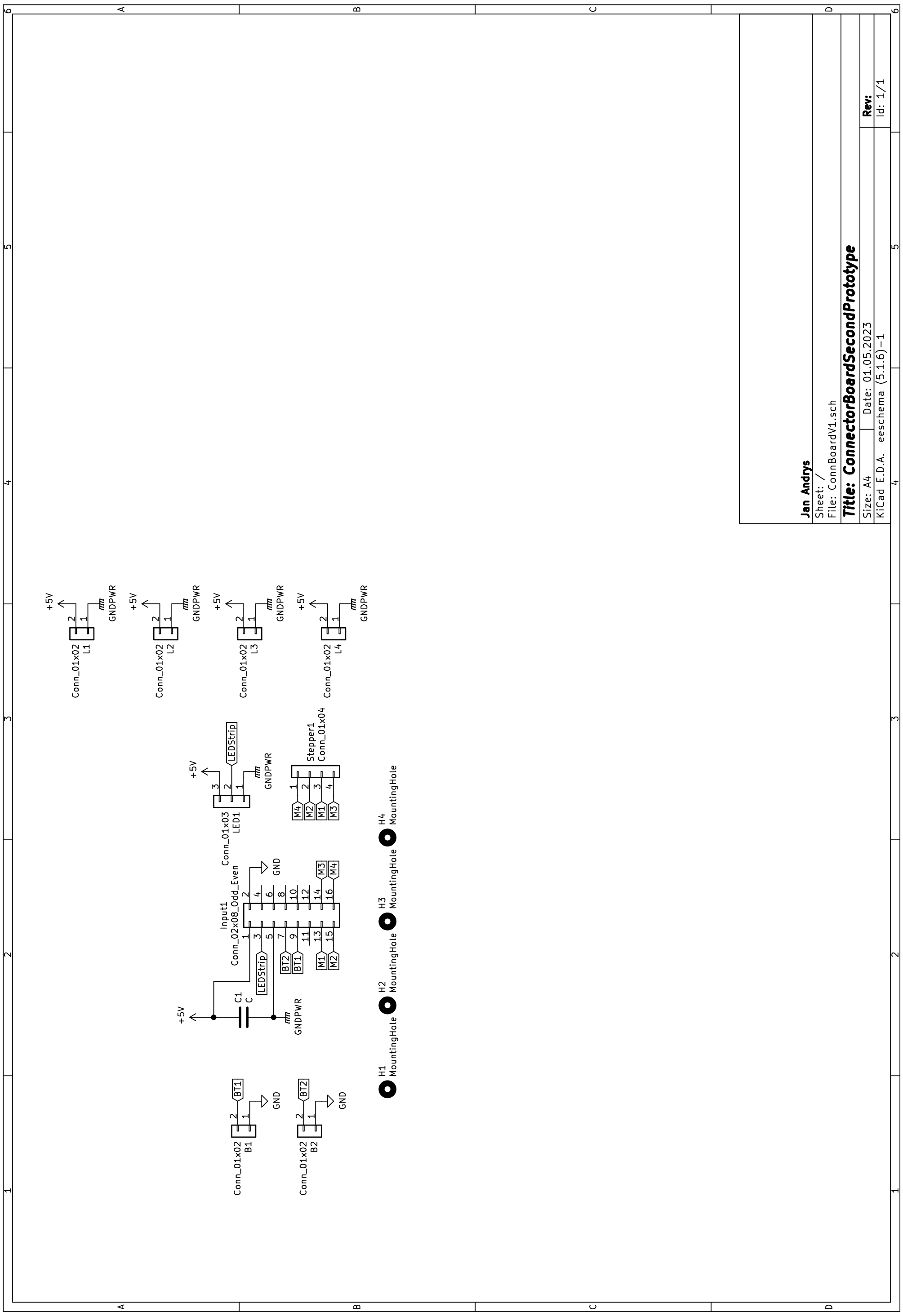

The second prototype – Connection board – Printed circuit board

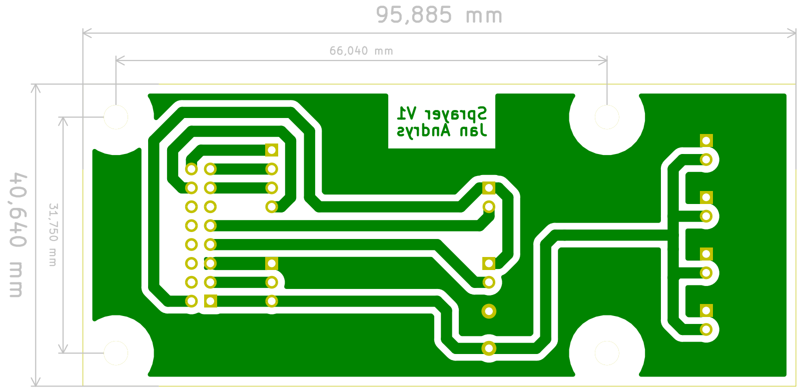

Appendix C
The second prototype - External Board

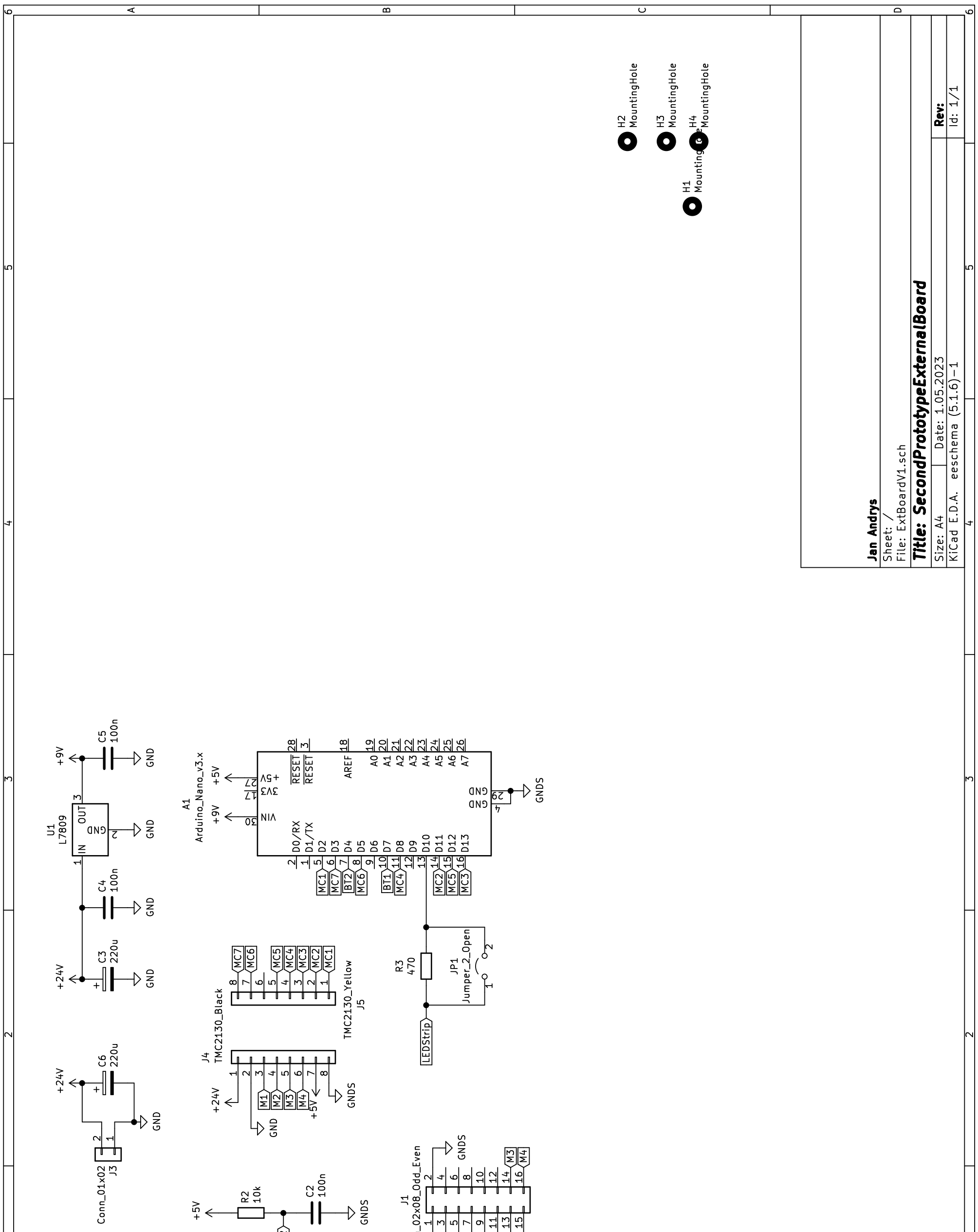

The second prototype – External board – Printed board circuit

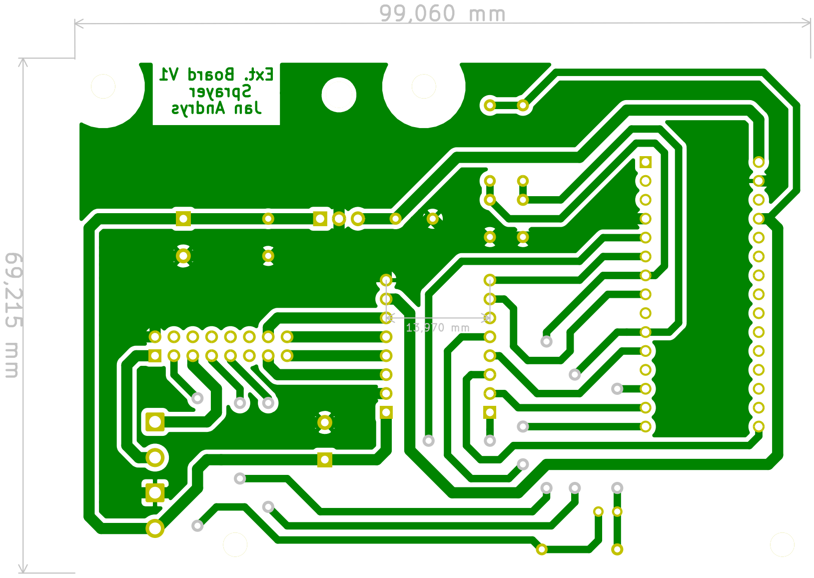

Appendix D
3D model of the second prototype